TWO-DIMENSIONAL LAMINAR FLOW OF NEWTONIAN AND NON-NEWTONIAN FLUIDS IN A T-CHANNEL

A DISSERTATION

Submitted in partial fulfilment of the

requirements for the award of the degree

of

INTEGRATED DUAL DEGREE

(Bachelor of Technology & Master of Technology)

in

CHEMICAL ENGINEERING

(With specialization in Hydrocarbon Engineering)

By

VINIT KHANDELWAL

DEPARTMENT OF CHEMICAL ENGINEERING
INDIAN INSTITUTE OF TECHNOLOGY, ROORKEE
ROORKEE-247667
JUNE-2013

Candidate's Declaration

I hereby declare that the work, which is being presented in the dissertation entitled **"Two-Dimensional Laminar Flow of Newtonian and Non-Newtonian Fluids in a T-Channel"** in the partial fulfilment for the requirements of the award of the Integrated Dual Degree (Bachelor of Technology & Master of Technology) in Chemical Engineering with specialization in "Hydrocarbon Engineering", submitted in the Department of Chemical Engineering, Indian Institute of Technology Roorkee, Roorkee, is an authentic record of my own work carried out during the period from May 2012 to June 2013 under supervision of **Dr. Amit Kumar Dhiman**, Assistant Professor, Department of Chemical Engineering, Indian Institute of Technology Roorkee, Roorkee.

I have not submitted the matter, embodied in this dissertation for the award of any other degree.

Date:

Place: Roorkee (Vinit Khandelwal)

Certificate

This is to certify that the above statement made by the candidate is correct to the best of my knowledge and belief.

Dr. Amit Kumar Dhiman
Assistant Professor
Department of Chemical Engineering
Indian Institute of Technology Roorkee
Roorkee - 247667 (India)

Acknowledgement

I express my deep sense of gratitude to my guide **Dr. Amit Kumar Dhiman**, Assistant Professor, Department of Chemical Engineering, Indian Institute of Technology Roorkee, Roorkee, for his keen interest, constant guidance and encouragement throughout the course of this work, his experience, assiduity and deep insight of the subject held this work always on a smooth and steady course.

Thanks are due to Dr. Vijay Kumar Agarwal, Professor and Head, Department of Chemical Engineering, Indian Institute of Technology Roorkee, for providing various facilities during this dissertation.

Above all, I want to express my heartiest gratitude to The Almighty, my parents (Mrs. Anita Gupta and Mr. Ramavtar Gupta), for their love, faith and support for me, which has always been a constant source of inspiration.

VINIT KHANDELWAL

Contents

List of Figures

List of Tables

Abstract

Flow behaviour of non-Newtonian shear-thinning fluids in a two-dimensional right angled horizontal T-channel are studied in the laminar flow regime. In particular, the numerical calculations are performed for the following range of physical parameters: Reynolds number (Re) = 5-200 and power-law index (n) = 0.2-1 (covering shear-thinning, n<1 and Newtonian fluids, n=1). The flow fields have been described by streamline contours. The engineering parameters such as recirculation length, critical Reynolds number for the onset of flow separation and the variation of viscosity along the lower wall of side branch are determined for the above range of settings. The results showed that the length of recirculation zone increases on increasing the Reynolds number and it also increases on decreasing the power-law index. The critical Reynolds number for the onset of flow separation decreases with decrease in power-law index (n).

PAPER COMMUNICATED IN JOURNAL

- Vinit Khandelwal, Amit Dhiman and Laszlo Baranyi, Two-dimensional laminar flow of non-Newtonian shear-thinning fluids in a T-channel.

.

International Journal of Engineering Sciences

Nomenclature

D	Non-dimensionalizing length scale, m
I_2	Second invariant of the rate of deformation tensor, s^{-2}
L_d	Side branch length, m
L_r	Length of recirculation region, m
L_1	Total length in mainstream direction, m
m	Power-law consistency index, Pa s^n
n	Power-law index, dimensionless
N_{cells}	Total number of cells in the domain
P	Pressure, Pa
Re	Reynolds number, $\mathrm{Re} = \frac{\rho D^n V_{avg}^{2-n}}{m}$
t	Time, s
U	Velocity along X-axis, m/s
V	Velocity along Y-axis, m/s
V_{avg}	Average velocity of the fluid at inlet, m/s
W_b	Width of side branch, m
W_c	Width of main branch, m
X_d	Downstream length of main branch, m
X_u	Upstream length of main branch, m
X	Coordinate in sidestream direction, m
Y	Coordinate in mainstream direction, m

Greek Symbols

ρ	Density of fluid, kg m^{-3}
δ	Minimum grid spacing, m
Δ	Maximum grid spacing, m
η	Power-law viscosity, Pa s
τ	Extra stress tensor, Pa
ε	Rate of deformation tensor, s^{-1}

Chapter 1. Introduction

Pipe networks are widely used to transport and convey fluids and gases. These networks may vary from fewer pipes to a complex assembly of very large number of pipes (e.g. network of water supply in a city, Fig. 1). Other than pipes, the network also consists of some additional components like bends, valves, elbows, expansions, contractions, T-junctions and many others. Presence of all these components in the pipe network may lead to boundary layer separation due to change in momentum of the flow caused by the pipe components.

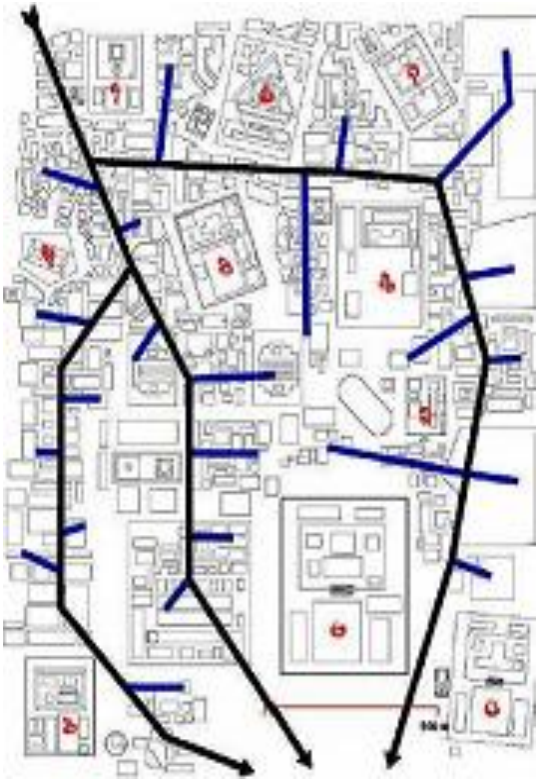

Figure 1: Layout of water distribution plan through a pipe network in city

Figure 2: Pipe network in industries for conveying fluids

A variety of flow configurations can exist for a pipe network. For geometry like a 45 degree branch, a 90 degree T-channel or a symmetric Y-channel, various flow configurations like bifurcating or combining flows are of main concern.

Diversion flows are present in a variety of natural as well as man-made environments like within cardiovascular systems in branched arteries, meander cut offs, river diversions and side-diversion channels. Mechanics of diversion flows are not well understood because of the complexity involved due to presence of non-uniform 3-D flow patterns that exhibits streamwise vortices and recirculation zones. The mechanics of this type of flow is of great interest to biomedical researchers for resolving the occurrence of thrombi (clotting of blood) and atherosclerotic plaque in branched arteries. This will also be of interest to hydraulic researchers and geomorphologists for examining bed-morphology. In order to solve these problems a thorough study of flow behaviour and shear stress variations in the vicinity of junction and solid walls of the channel is required.

Another aspect of flow in a bifurcating channel that has achieved wide attention is the phase separation in branches because of its importance in wet steam distribution in enhanced oil recovery and also in power plants.

In the current study we are mainly concerned with a very small but extremely important component of pipe network: T-channel. A T-channel is amongst the most common component in pipe networks and is mainly used to gather fluid from many pipes to a single pipe (converging flow) or to divide a single flow stream into several branches (diverging flow). The following figure depicts several possibilities (viz. dividing flow and converging flow) of fluid flowing through a T-channel.

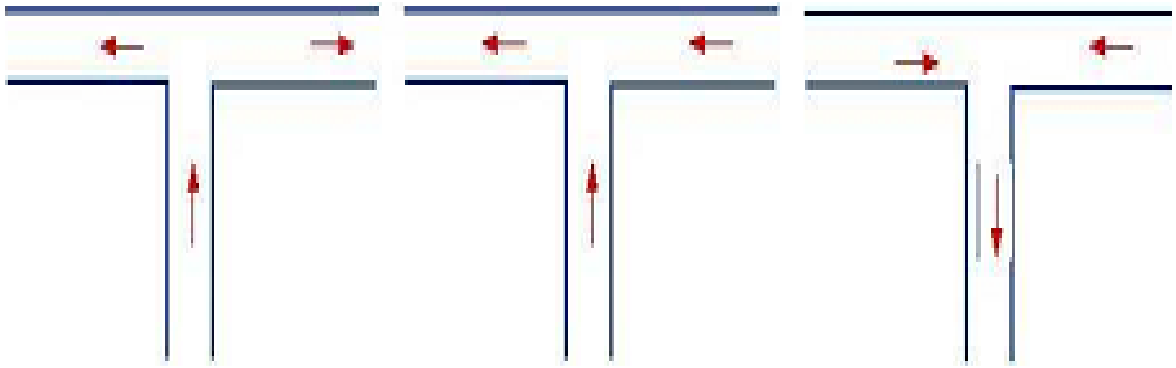

Figure 3: Various possible fluid flow configurations in a T-channel

Figure 4 shows a schematic representation of 2-D flow observed in bifurcating flows having side branch at right angle to the main branch. When the fluid reaches the junction, it gets laterally accelerated due to the influence of suction pressure at the exit of the side branch. This result in the division of main branch flow stream into two sub streams such as a part of the main flow enters the side branch whereas the remaining fluid goes downstream of the main branch.

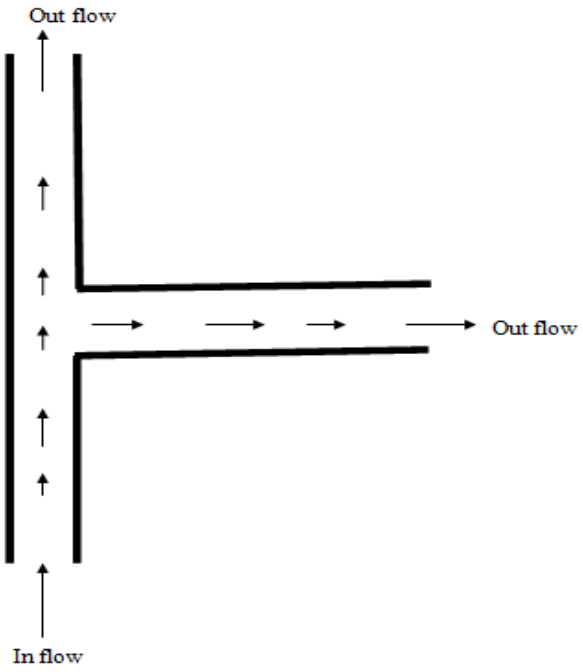

Figure 4: A schematic diagram of fluid flow in a bifurcating T-channel

In environmental and hydraulic engineering, one often encounters the flow in branched channels. Depending on the outflow and inflow conditions and directions, the flow behaviour of the fluid at the junction also changes.

A recirculation zone near the junction along the left wall of the main branch, another recirculation zone is seen to occur in the side branch, and one stagnation point at the downstream corner of the junction are the main flow characteristics of fluid flow in a dividing channel. In the downstream of the channel in the main branch direction, towards the far solid wall, flow separation may also occur because of flow expansion [1].

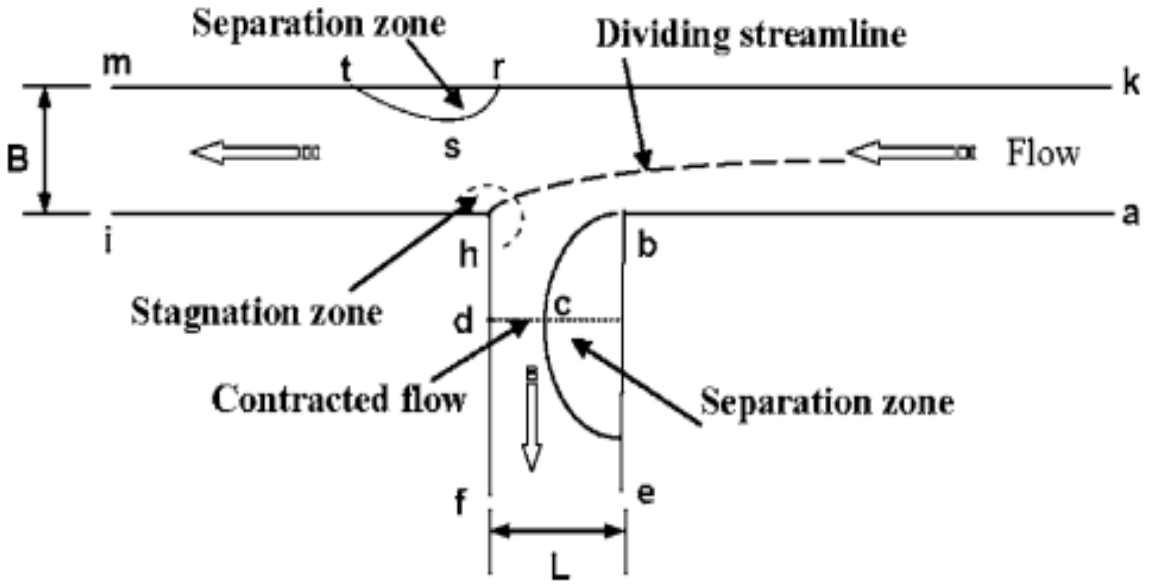

Figure 5: Flow characteristics of bifurcating flow in T-channels (Ramamurthy et al. [1])

In the region around the junction the transverse pressure gradients induce an area of mean-velocity gradients, depth-varying surface of flow bifurcation and separation, vortices, and zone of reverse flows. When the fluid reaches the junction it gets divided in two streams and the bifurcated flow generates instability. Neary et al [2] found it to be because of transverse pressure gradient and centrifugal and shear forces depicting a clockwise secondary motion cell. Thus, due to the action of centrifugal force at the junction and change in the direction of flow of fluid formation of recirculation region in the side branch takes place.

Two main aspects are there common to the flow situation under consideration and these are a result of sudden change in the direction of flow. These features are:

(i) flow detachment and development of recirculation region along the mainstream direction of flow, and

(ii) recirculation zones generating in a branch which is at right angle with mainstream direction of flow.

For a ninety degree branch, a weak recirculation region may also get induced in the main branch because of the fluid passing via side branch. This aspect of generating secondary velocities is more prominent in curved pipes and ducts because centrifugal forces are

sustained in those geometries and may even make difficult to examine the flow in 2-D. But for a right angled branch this force is small in magnitude and is only observed near the junction when the fluid is just about to enter the side branch. With appropriate flow conditions the developed recirculation zones decays in the downstream direction of the branch towards the outlet. In experiments simulating two-dimensional conditions (i.e. rectangular ducts with large aspect ratio) the secondary flow is thought to arise only after a threshold Reynolds number.

1.1 Motivation

Although a plethora of studies in dividing flows have been conducted so far, it seems that because of the high complexity involved in their mechanics, a lot more research has to be done in order to to correctly predict their complex behaviour and completely understand their flow characteristics. The need for investigating this kind of flow arises from the fact that this not only is encountered in countless engineering and research applications but is also of significant importance in biomedical and hydraulic practice as well as to geomorphologists for examining the bed morphology.

The fluid flow in a T-channel is characterized by the following observations: a recirculation region along the bottom wall of the branched channel when the flow enters the side branch, another recirculation region along the left wall of the main branch of the T-channel at the junction, and a stagnation point at the corner which is downstream of the junction. Recirculation zone can be defined as the areas of recirculating fluid with extremely low velocities; thus it has a significantly high sediment deposition potential. Continuous sediment deposition over a period of time reduces the conveyance of the channel.

Therefore, in engineering practice, it is very necessary to investigate the general flow behaviour in reattaching and recirculating flows. Flow through a T-channel is found to have a plethora of engineering applications in irrigation systems, wastewater treatment, flood water driving, biomechanical application, phase separation, oil and gas industry, polymer and pharmaceutical industry, and in many other areas.

Flow in a T-channel for Newtonian fluids have been examined extensively both numerically as well as experimentally to gather the basic information of flow in reattaching and recirculating flows in the laminar flow regime. The current study aims to investigate two-

dimensional laminar flow for Newtonian and Non-Newtonian fluids in a T-channel for a broad range of Reynolds number. However, before going into an in-depth presentation and analysis of the problem, it will be useful to account in brief the current status of the literature to the problem under consideration.

Chapter 2. Literature Review

A large portion of the available literature for flow of fluid through a T-channel deals with high Reynolds number side of Newtonian fluids where the core objective has been to examine in detail the recirculation and reattachment phenomena. In contrast, very less investigation has been conducted for examining the flow characteristics of non-Newtonian fluids at low Reynolds number.

Grace and Priest [3] performed an experimental study for dividing flows at several aspect ratios of the branch channel orientation to the main channel. There were two regimes in which the division of flows have been classified, one with and another without the existence of local standing waves in the vicinity of junction. Froude number was found to be small in the region that where standing waves doesn't exist. For the case of no standing waves, the branch-to-downstream aspect ratio and downstream-to-upstream aspect ratio were almost tending to unity and the ratios slightly decreased whereas the upstream discharge ratio of branch-to-main channel increased. Law and Reynolds [4] examined the bifurcating flows via experimental and analytical methods and came with a conclusion that for a bifurcating flow at low Froude numbers, the energy and momentum principles can both be used to visualize the flow in the extension of the main channel.

Hayes et al. [5] performed a study to examine the flow behaviour of Newtonian fluid in a planar two-dimensional (2-D) T-branch for Reynolds number range (10-800). This was studied for two different outlet boundary conditions: (a) constant equal exit pressure, and (b) specified flow split at the outlet of the branches. They found that the fractional flow of fluid in the downstream of the main branch increases with Reynolds number when equal pressure at the exit of both branch is applied and when specified flow split was imposed at the outlet of each branch, the intensity and size of recirculation region enhances as more fluid goes into the side branch. The critical Reynolds number after which the onset of recirculation regions begin in the side branch increases on decreasing side branch width and on increasing fractional flow in side branch.

Neary and Sotiropoulos [6] presented numerical solutions for steady 3-D laminar fluid flow in ninety degree rectangular cross-sectional diversions for Reynolds number range (496-525), duct aspect ratios (1-8) and discharge ratios (0.23-0.64). They compared solutions with experimental measurements to elucidate flow topology patterns and showed that both size of

the recirculation zone decrease on increasing the discharge ratio. They also showed that for ducts with large aspect ratio, the bottom and top solid boundaries significantly affects the flow at the symmetry plane.

Weber et al. [7] experimentally investigated ninety degree open channel geometries with combining flows of equal widths for Reynolds number ranging from 500 to 1000. They performed depth measurements using a point gauge while for the case of velocity measurements Acoustic Doppler Velocimetry was used for a grid that was defined throughout the junction region. They also gave a very wide data set which comprised of water surface mappings, turbulence stresses and three velocity components. Huang et al. [8] performed a detailed study for numerically examining three-dimensional (3-D) turbulence model for converging flows in open-channels for Reynolds number range (500-1000) and subsequently they validated their model from the broad test data provided by Weber et al. [7].

Ramamurthy et al. [1] studied open-channel laminar and turbulent 3-D flow characteristics of a 90° rectangular channel junction of equal width over a range of discharge ratio (0.149-0.838). They developed a (k-ω) turbulence model for investigating the characteristics of flow in bifurcating open-channels. They also presented a data set consisting of water surface mappings and 3-D velocity variations around the junction of the channel. They performed depth measurements using point gauges, while Laser Doppler Anemometer was used for obtaining velocity measurements over grids defined throughout the junction. They showed that the energy and momentum coefficients based on the three-dimensional model presented in their study yield more realistic momentum transfers and energy losses for bifurcating flow configurations.

Shamloo and Pirzadeh [9] investigated the characteristics of recirculation zones that develop in a T-channel over a range of discharge ratios (0.2-0.8) by using FLUENT software. They performed a numerical study using RSM turbulent model and the results of velocity field measurement which were obtained by using the k-ε Standard model were compared with the results presented by Shettar & Murthy [10]. Dimensions of recirculation zones were measured and compared with the results of Kasthuri & Pundarikanthan [11] by using RSM turbulent model.

Mathioulakis et al. [12] studied experimentally as well as numerically the flow in a ninety degree square duct bifurcation for equal branch flow rates and for Reynolds number of 1200. They carried out velocity measurements with a one-component Laser Doppler

Velocimeter, besides the time mean streamwise velocity component, its time variation due to vortex shedding which took place in the extension of the main duct, as well as secondary flow velocities in the ninety degree branch. The experimental data were compared with the results of a numerical method, constituting an extension of the well-known SOLA method to a three-dimensional generalized coordinate system. These comparisons were successful in the vertical branch but less satisfactory in the horizontal branch where unsteadiness was very strong. They predicted the characteristic frequency of the velocity fluctuations in the detached shear layer of the horizontal branch very well but the velocity amplitudes were underestimated. The predicted secondary flow in the vertical branch was compared with the experimental data presenting maximum values close to the inlet mean velocity.

Yanase et al. [13] investigated laminar flow in a curved rectangular duct for a range of the aspect ratio (1-12) using spectral method and found five branches of steady solutions. They also investigated linear stability characteristics for all the steady solutions and found that one steady solution is linearly stable for most of the aspect ratio, but two linearly stable steady solutions exist for a region of small aspect ratio and there are several intervals of aspect ratio where there is no linearly stable steady solution.

In addition to flow characteristics for a Newtonian fluid, Liepsch et al. [14] studied laminar flow in a plane ninety degree bifurcation for non-Newtonian fluids for a range of Reynolds number (496-1130) and discharge ratio (0.23-0.64). They developed velocity profiles as a function of flow rate ratio, Reynolds number and geometry and compared it with Laser Doppler Anemometry measurements. The shear stresses and circulation patterns were examined keeping in view of the available data for formation of atherotic plaques in human circulatory system. They also presented calculations beyond the range of measurements which might be a value to biomechanics.

Bramley and Dennis [15] studied numerically 2-D steady flow of viscous incompressible fluid in a branching channel for Reynolds number (100, 500, 1000 and 2000). The downstream and upstream boundary conditions were discussed and a logarithmic transformation was applied to the coordinate measuring distance downstream in order to extend the numerical solution far enough downstream. They presented numerical methods for tackling singularity in vorticity at the sharp corners of the junction. They also discussed the effect of variation of Reynolds number and the relative channel width downstream and upstream of the branch on flow separation.

Ehrlich and Friedman [16] investigated dividing flows for biomedical applications in 2-D regions and mapped the radiographs of arteries on rectangles via a slit. Initially they approximated wall shapes via cubic splines, but wall vorticities were found to be highly sensitive with variation in curvature. As a result of this least squares polynomial were approximated in place of the splines. They also developed correlations between shear rates and computed wall vorticities from the results available through laboratory experiments.

Miranda et al. [17] examined Newtonian fluids for steady as well as unsteady flow regimes for a range of Reynolds number (10-1000) and discharge ratio (0.1-0.9) in a dividing geometry and compared results for shear stresses with the simulations and experimental measurements of Liepsch et al. [14] and Khodadadi et al. [18,19], Khodadadi [20]. They investigated a particular case of non-Newtonian flow and left open a route of examination dealing with the investigation of other flow characteristics in a channel, such as the effect of shear-thinning tendency on the flow behaviour in the vicinity of the junction.

Benes et al. [21] numerically dealt with laminar as well as turbulent flows of Newtonian and non-Newtonian fluids in bifurcating branched channels for discharge ratio (0.25 and 0.75). For the turbulent case they used the Explicit Algebraic Reynolds Stress Model (EARSM) and showed that this model is capable of capturing secondary flows in channels of rectangular cross-section. For the case of laminar flow of non-Newtonian fluid numerical results were presented. Further for the case of turbulent flow through channels having branch at right angle, simulations were done.

Moshkin and Yambangwi [22] developed a computational method for solving start-up flow in a T–channel with viscous incompressible fluid for Reynolds number range (10-400). They studied the effect of flow rate and curvature ratio of planar U-bend channel and concluded that the size of recirculation region increases with decreasing curvature ratio and increasing flow rate. The flow initially at rest was driven by fixed pressure drops applied suddenly across the exits and entries of the T-channel. They also presented the predicted variations of flow patterns and the volumetric flow rates with time for different pressure drop values. It was shown that before approaching steady state distribution the start-up flow passes through different flow direction.

Recently, non-Newtonian laminar fluid flow in steady as well as unsteady regime in a 2-D T-junction was studied by Matos and Oliveira [23] for the following range of parameters: Reynolds number (50-1000) and power-law index (0.1–1). They found that on increasing the

flow rate ratio, the maxima of shear stress increases with but the location of maxima changes. For small discharge ratios the maximum magnitudes occur in the main branch, where stretching occurs and where more amount of fluid exists, while for large discharge ratios they occur in the side branch.

Thus, after going through the current status of literature study of the problem under consideration, we can sum up that adequate information is present in the literature on the Newtonian and non- Newtonian flow through a T–channel at high Reynolds numbers region. However, despite of having plethora of engineering applications, the non-Newtonian shear–thinning flow through a T–channel has not been investigated in the literature at low Reynolds numbers. So, the main aim of this study is to examine the characteristics of non-Newtonian flow for the range of conditions: Reynolds number (Re) = 5–200 and power-law index (n) = 0.2–1 (covering shear- thinning, $n<1$ and Newtonian, $n=1$ fluids). Another main objective of the current study is to determine the critical Reynolds number at which onset of flow separation occurs.

Chapter 3. Problem Statement and Numerical Solution Methodology

The 2D, incompressible and laminar flow of non-Newtonian shear-thinning fluids through a T-channel is schematically displayed in Fig. 6. The channel inlet of width $W_c = D$ (also the non-dimensionalising length scale) has been exposed to a fully developed velocity field with an average velocity of V_{avg} at the inlet of main branch of the channel (also the non-dimensionalising velocity scale). The upstream length ratio between the inlet and the junction of the channel (X_u/D) is taken as 10, and the downstream length ratio between junction and the exit plane (X_d/D) is taken as 30 with the total length ratio of the main channel being L_1/D=41. The non-dimensional length of side branch (L_d/D) is taken as 25. These length ratios were chosen in the following manner.

For determining the influence of the domain under consideration, especially towards the high Reynolds number end, simulations were conducted at Re=200 for Newtonian fluids (n=1) and side branch length ratios of 20, 25, 30. The influence of side branch length ratio on the recirculation length is presented in Table 1. The relative difference in the reattachment length for length ratios of 25 and 30 was found to be about 3.21%, while for the case of maximum shear-thinning behaviour (n=0.2), the relative difference in reattachment length for length ratios of 25 and 30 was found to be about 3.72%. This was felt to be small enough to justify the choice of a side branch length ratio of 25 for subsequent simulations. Similarly, the change in the recirculation length for the downstream length ratios of 25, 30 and 35 at Re=200 is presented in Table 2. The relative difference in reattachment length ratio for 30 and 35 is found to be about 1.70%, while for the case of maximum shear-thinning behaviour (n=0.2), it was seen to be about 3.46%. So, a side branch length ratio of 30 is finalized for subsequent computations. Similarly, the change in the recirculation length for the upstream length ratios of 5, 10 and 15 at Re=200 is presented in Table 3 and the corresponding difference in reattachment length ratio for 10 and 15 is found to be less than 0.40%, while for the case of maximum shear-thinning behaviour (n=0.2), it was found to be about 1. 02%. Thus, an upstream length ratio of 10 has been employed in all the further computations.

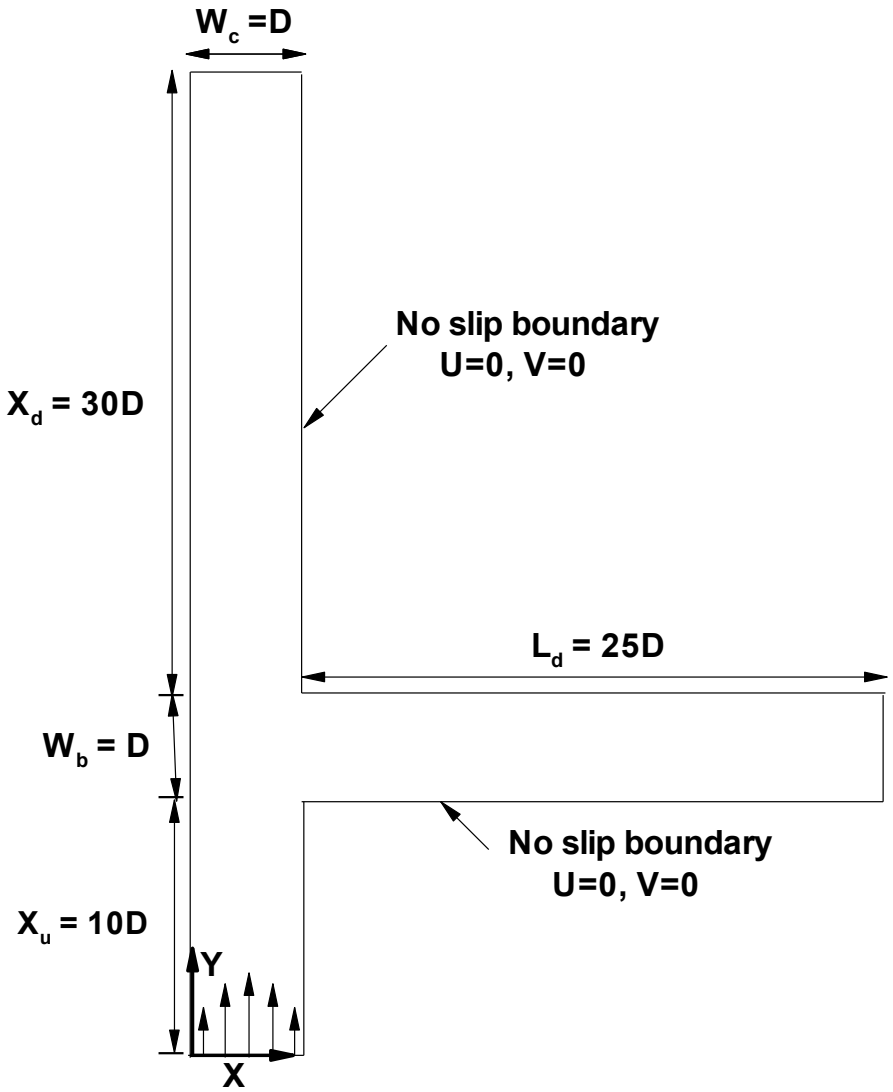

Figure 6: Schematic diagram of flow geometry in the current study

Table 1: Influence of side branch length (L_d/D) on recirculation region length (L_r/D) at Reynolds number (Re) = 200

L_d/D	N_{cells}	n=1		n=0.2	
		L_r/D	% error	L_r/D	% error
20	149625	4.07085	7.09128	9.28827	7.561512
25	154875	3.92329	3.20944	8.95672	3.722044
30	160125	3.80129		8.63531	

Table 2: Influence of downstream length (X_d/D) on recirculation region length (L_r/D) at Reynolds number (Re) = 200

X_d/D	N_{cells}	n=1		n=0.2	
		L_r/D	% error	L_r/D	% error
25	149625	3.80327	4.70503	8.51367	8.24036
30	154875	3.92329	1.6978	8.95672	3.46521
35	160125	3.99105		9.27823	

Table 3: Influence of upstream length (X_u/D) on recirculation region length (L_r/D) at Reynolds number (Re) = 200

X_u/D	N_{cells}	n=1		n=0.2	
		L_r/D	% error	L_r/D	% error
5	149625	3.94183	0.86514	9.13382	3.02389
10	154875	3.92329	0.39073	8.95672	1.02631
15	160125	3.90802		8.86573	

For a 2-D, incompressible, laminar flow, the equations of continuity, the dimensionless *X*- and *Y*-components of Cauchy's equations are given below [24, 25].

Continuity:

$$\frac{\partial U}{\partial X}+\frac{\partial V}{\partial Y}=0 \tag{1}$$

X- Momentum:

$$\frac{\partial U}{\partial t}+U\frac{\partial U}{\partial X}+V\frac{\partial U}{\partial Y}=-\frac{\partial P}{\partial X}+\frac{1}{\mathrm{Re}}\left(\frac{\partial \tau_{XX}}{\partial X}+\frac{\partial \tau_{YX}}{\partial Y}\right) \tag{2}$$

Y- Momentum:

$$\frac{\partial V}{\partial t}+U\frac{\partial V}{\partial X}+V\frac{\partial V}{\partial Y}=-\frac{\partial P}{\partial Y}+\frac{1}{\mathrm{Re}}\left(\frac{\partial \tau_{YX}}{\partial X}+\frac{\partial \tau_{YY}}{\partial Y}\right) \tag{3}$$

For the case of an incompressible fluid, the extra stress tensor (which is symmetric, $\tau_{ij} = \tau_{ji}$) can be related to the rate of deformation tensor (ε_{ij}) as

$$\tau_{ij} = 2\eta\varepsilon_{ij}$$

The components of the rate of strain tensor are correlated to that of velocity as follows:

$$\varepsilon_{XX} = \frac{\partial U}{\partial X}; \quad \varepsilon_{YY} = \frac{\partial V}{\partial Y}; \quad \varepsilon_{XY} = \varepsilon_{YX} = \frac{1}{2}\left(\frac{\partial U}{\partial Y} + \frac{\partial V}{\partial X}\right)$$

The viscosity (η) for a power-law fluid is defined as

$$\eta = m\left(\frac{I_2}{2}\right)^{\frac{n-1}{2}}$$

Here m is the power-law consistency index which is used to determine the viscosity of the fluid; n is the power-law index. Clearly, n=1 implies the ideal Newtonian flow behaviour; n<1 implies shear-thinning fluid behaviour and the values of n as small as 0.2-0.3 are very common for particulate slurries and polymeric systems. Thus, the range of setting of the power-law index $0.2 \leq n \leq 1$ used in current study is driven by the behaviour of industrially important fluids. I_2 in the above equation is the second invariant of the rate of deformation tensor and is given by

$$I_2 = \sum\sum \varepsilon_{ij}\varepsilon_{ji} = 2\left(\varepsilon_{XX}^2 + \varepsilon_{XY}^2 + \varepsilon_{YX}^2 + \varepsilon_{YY}^2\right)$$

The only dimensionless group present in above equations is Reynolds number and is defined as follows:

$$\mathrm{Re} = \frac{\rho D^n V_{avg}^{2-n}}{m}$$

The dimensionless boundary conditions for the flow configuration under consideration may be written as follows (Fig. 6):

- At the inlet boundary: The fully developed velocity profile for power-law fluids in the laminar flow regime in a channel is given as

$$U = 0;\ V = \left(\frac{2n+1}{n+1}\right)V_{avg}\left[1-\left(\left|1-\frac{2X}{D}\right|\right)^{\frac{n+1}{n}}\right] \text{ for } (0 \leq X \leq D)$$

- At the left and right boundary walls of main branch:

$U = 0\,;\ V = 0$ (no slip condition)

- At the upper and bottom walls of side branch:

$U = 0\,;\ V = 0$ (no slip condition)

- At the outlet boundary of main and side branch: The default pressure outlet condition (both exits exposed to atmosphere) available in ANSYS is used, i.e., zero gauge pressure at both the exits.

3.1. Numerical Solution Methodology

The grid arrangement used for examining the flow in a T-channel is depicted in Fig. 7. The grid is built via Gambit which is a pre-processor of Ansys Fluent, and displays the complete grid arrangement for total domain under consideration (Fig. 7) along with a magnified display of the non-uniform orthogonal grid structure (Fig. 8). Our computational domain has both uniform as well as non-uniform meshing with a fine clustering of control volumes in the area of sharp gradients and a coarse meshing where the gradients are low. The junction of the channel where the flow diversion takes place is a zone of utmost consideration where significant gradients in flow velocity may occur. For overcoming this problem, a very fine meshing is used in this region. In order to clearly understand the physics of the flow separation in the side branch a very fine meshing has been done up to a distance of 5D. The rest is a non-uniform mesh which subsequently gets coarser on going away from the junction in both upstream and downstream directions, such that in the vicinity of the junction the smallest control volumes is present while the largest control volumes are away from the junction.

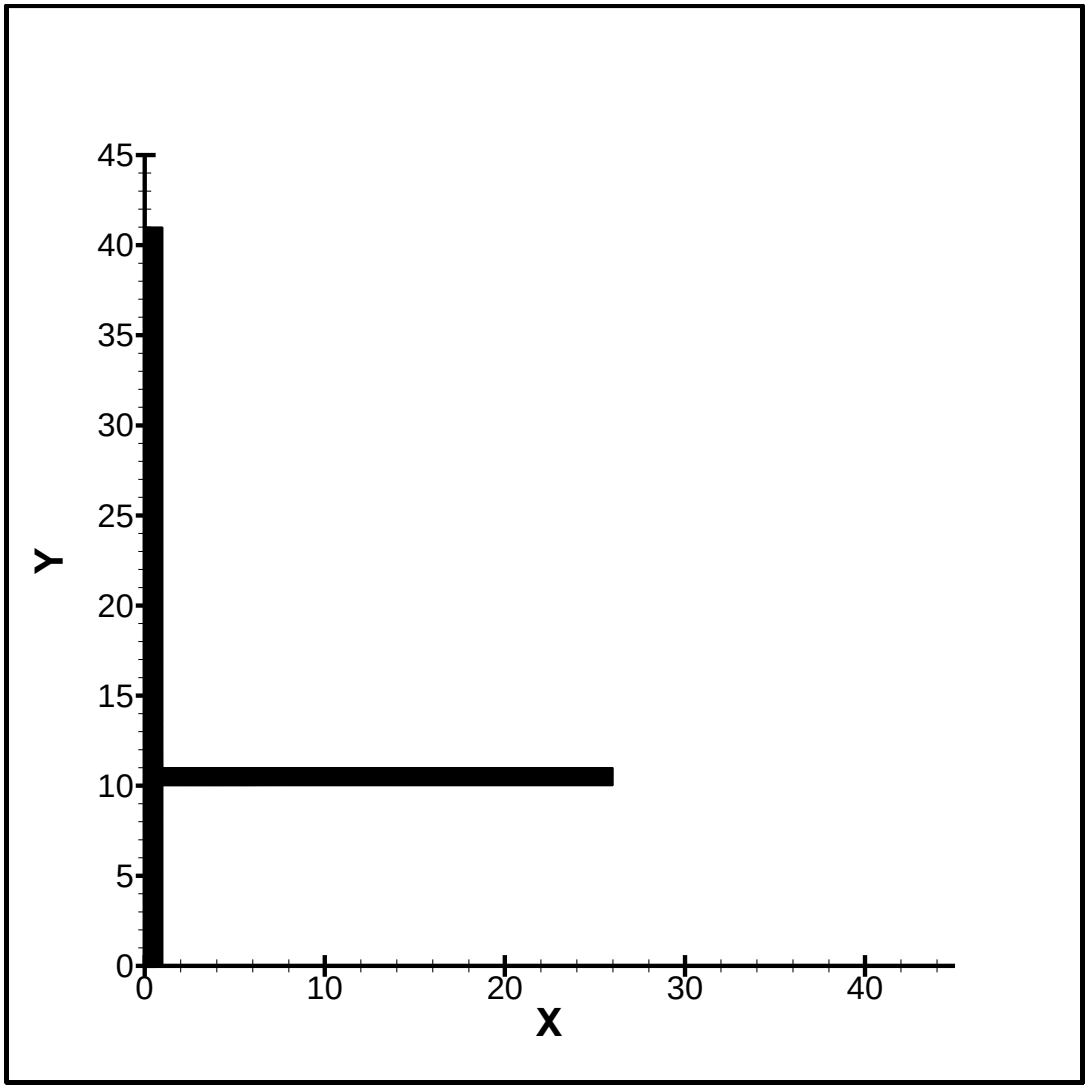

Figure 7: Complete view of grid structure for the flow of fluid in a T-channel

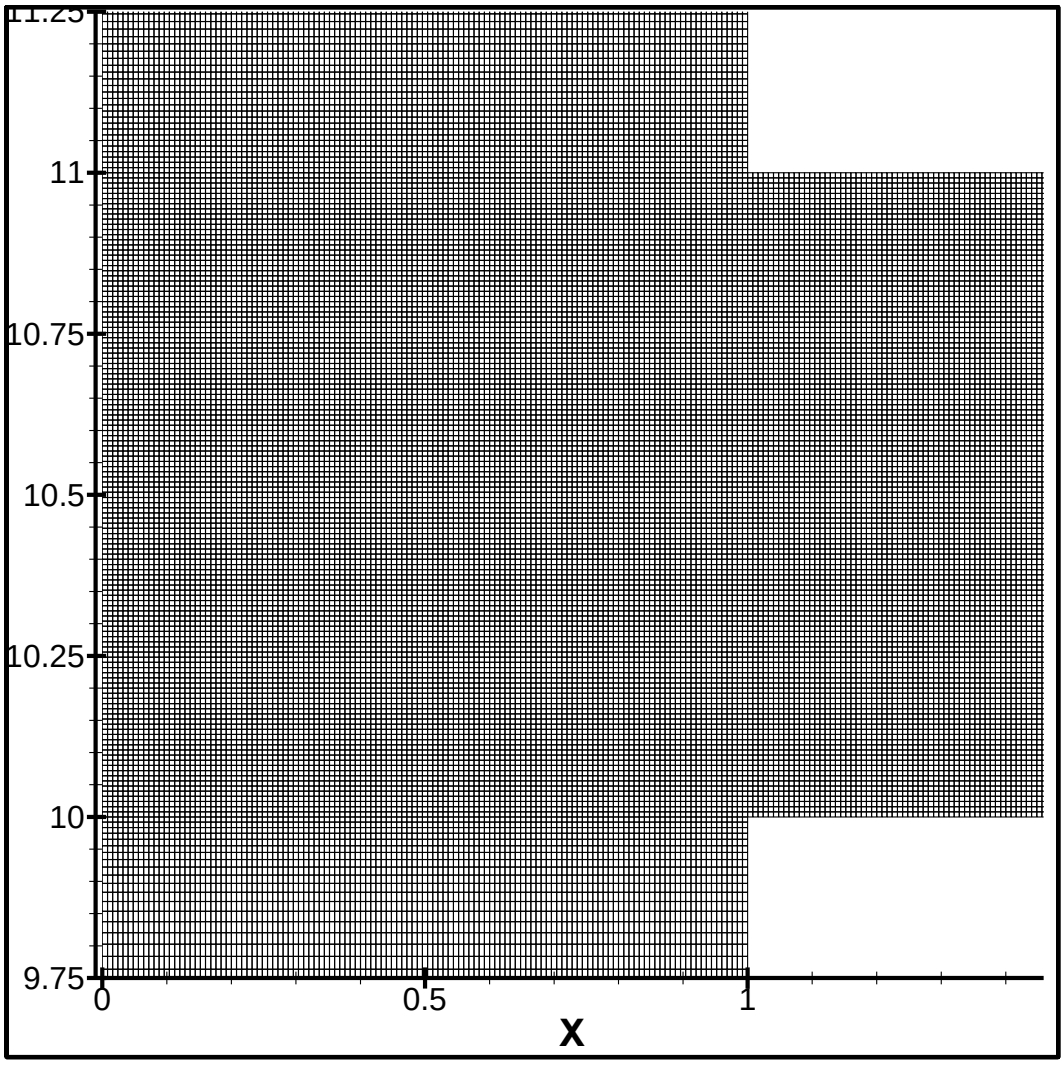

Figure 8: Magnified view of a non-uniform grid structure at the junction for the flow of a fluid in a T-channel

It is important to analyse the effect of grid fineness on the physical parameters. A detailed investigation of sensitivity of the obtained computational results with respect to the grid fineness and number of elements for every case has been conducted using three different grids with 106500, 154875 and 254007 number of cells of different fineness and the results have been shown in Table 4. The minimum grid spacing (δ) at junction and in the region around the junction along the side branch for the three grids is 0.01D, 0.008D and 0.006D respectively and the maximum grid spacing is Δ=0.5D at distance far off from the junction is seen to be decently resolving the flow characteristics in a T-channel. For stretching the cell sizes from minimum to maximum grid spacing in both *X*- and *Y*-directions, first length function in employed.

The percentage relative difference in the value of reattachment length for Newtonian fluids (n=1) for the case of Re=50 is found to be about 0.10% for the grid having 106,500 cells and about 0.005% for the grid having 154,875 cells in comparison to the grid having 254,007 cells. For the case of maximum shear thinning behaviour (n=0.2) at Re=50, the percentage relative difference in the value of recirculation length is found to be about 2.20% for the grid having 106,500 cells and about 0.78% for the grid having 154,875 cells in comparison with the grid having 254,007 cells. Similarly, at Re=100, the corresponding percentage relative difference for Newtonian fluids (n=1) is seen to be about 0.08% for the grid with 106,500 cells and about 0.01% for the grid having 154,875 cells in comparison with the grid having 254,007 cells. For the case of maximum shear thinning behaviour (n=0.2) at Re=100, the percentage relative difference in the value of reattachment length is found to be about 1.92% for the grid having 106,500 cells and about 0.69% for the grid having 154,875 cells in comparison with the grid having 254,007 cells. And at Re=200, the percentage relative difference for Newtonian fluids (n=1) is found to be about 0.05% for the grid having 106,500 cells and about 0.01% for the grid with 154,875 cells in comparison with the grid having 254,007 cells, respectively. For the case of maximum shear thinning behaviour (n=0.2) at Re=100, the percentage relative difference in the value of recirculation length is found to be about 2.33% for the grid having 106,500 cells and about 1.30% for the grid having 154,875 cells in comparison with the grid having 254,007 cells. Thus, a grid size of 154,875 cells has been used in the present work.

Table 4: Sensitivity analysis for the flow through a T-channel at different values of Re

Grid Details			L_r/D					
			n=1			n=0.2		
Grid	N_{cells}	Δ	Re=50	Re=100	Re=200	Re=50	Re=100	Re=200
G1	106500	0.01	1.89324	2.66488	3.92168	3.22376	5.51387	8.79226
G2	154875	0.008	1.89512	2.66655	3.92329	3.27039	5.58264	8.95672
G3	254007	0.006	1.89521	2.66687	3.92372	3.29639	5.62173	9.07416

The current study has been conducted using the commercial software package Ansys Fluent via finite volume method. In order to investigate the flow characteristics on the collocated grid arrangement a two-dimensional, laminar, segregated solver was used. Simulations were conducted for constant density and the non-Newtonian power-law viscosity models. For discretising convective terms in momentum equation 2^{nd} order upwind scheme was used. In order to solve the pressure-velocity decoupling SIMPLE scheme was employed. In Ansys Fluent Gauss Siedel point by point iterative method in conjunction with AMG solver are used for solving the system of algebraic equations. When there is a very fine grid using AMG model could be highly beneficial because it significantly reduces the iterations and so the time taken by CPU to arrive at a converged result. The relative convergence criteria of 10^{-9} for the continuity, and *X*- and *Y*-components of the velocity are prescribed in the steady regime. For detailed investigation of flow characteristics in the T-channel unsteady simulations have also been run for the highest values of Re and extreme values of *n* (i.e., Re=200, *n*=1 and 0.2) with relative convergence criteria of 10^{-20} for the continuity, and *X*- and *Y*-components of the velocity.

Chapter 4. Results and Discussion

Analysis of the current available literature indicates that the flow behaviour of the problem under consideration depend on five parameters which are as follows: the flow index (n), the Reynolds number (Re), the dimensionless width of main channel (W_c/D), the dimensionless width of side branch (W_b/D) and the flow split or the discharge ratio. Because a several governing parameters are needed to fully characterise the flow system, but a detailed investigation of all combinations of parameters is not feasible. However, computations can be done for any random selection of the above parameters, the main objective in this study is to come up with such results so as to demonstrate the effects of Re and n on the flow characteristics. In particular, fluid flowing through a T-channel with $W_c = W_b = D$ is considered here. The results are presented for Reynolds number up to 200 and for n = 0.2, 0.4, 0.6 and 1, thereby covering both shear-thinning and Newtonian behaviours. The case of n = 0.8 has not been taken up in this study because the behaviour of fluid for this case is almost the same as that for Newtonian fluids (n = 1). The non-Newtonian behaviour is more predominant at power-law index (n) values considerably less than 1.

4.1. Validation of results

The results obtained after numerically solving the problem under consideration have been bench-marked with available results for the flow of Newtonian fluids in a T-channel. The validation of reattachment length for Newtonian fluids on varying Reynolds numbers has been presented in Fig. 9. The minimum percentage deviation of recirculation length found from this study in comparison to that given by Hayes et al. [5] is found to be about 0.23% whereas the maximum deviation is around 3.24%. Overall, the comparison between the two sets of results is found to be satisfactory, except for higher Reynolds number (Re= 200, for instance) where the two results seem to differ by about 3.24%.

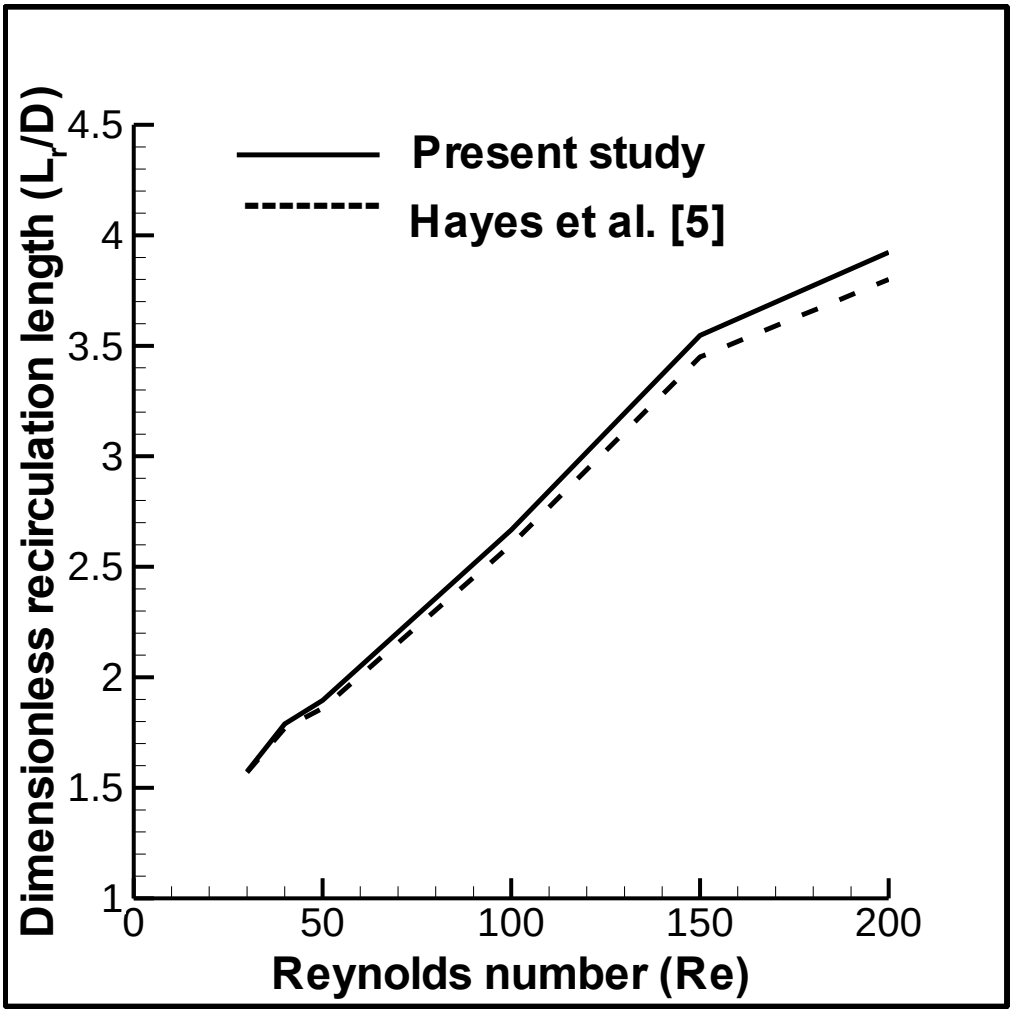

Figure 9: Validation of reattachment length with that of Hayes et al. [5] for n=1 at different values of Re

Furthermore, the general validity of the code has been compared for the critical Reynolds number at which the onset of boundary layer separation takes place for Newtonian fluids in a T-channel. The flow detachment from the bottom wall of the side branch is seen to begin at Re=17 for the case of Newtonian fluids. One similar experimental study was conducted by Karino et al. [29] and Karino and Goldsmith [30] and their results showed the onset of flow separation in the side branch of T-channel occurs at Re=18. Thus the results from the current study when compared with the results available in the literature seem to match satisfactorily. This further assures the reliability and accuracy of the employed numerical solution procedure.

4.2. Flow patterns

Figures 10-13 present representative flow patterns by way of streamlines in vicinity of the junction of T-channel for Re = 5, 30, 50, 100, 150 and 200 respectively. To ensure an extensive study of the variation of the power-law index (n) on the flow behaviour, four cases (n=1, 0.6, 0.4 and 0.2) have been demonstrated for the complete range of Reynolds number considered. It is worthwhile to mention here that the flow remains steady for the range of settings discussed in this work. Figure 10 shows the flow patterns of Newtonian fluid (n = 1) in a T-channel. For the case of Newtonian fluids, no recirculation zone is seen to occur in the side branch till Re = 16. The fluid while travelling to side branch from main branch maintains contact with the wall of the side branch. On increasing the Reynolds number, after a critical point the fluid gets separated from the bottom wall of the side branch and a recirculation zone is developed. The discussion on the onset of boundary layer separation at different values of n is given in section 4.4. After reattaching to the bottom wall of the side branch the flow regains its fully developed behaviour. On gradually increasing the Reynolds number (Re > 16), the size of recirculation region increases. The flow patterns for the Newtonian fluids in a T-channel are found to be in close agreement with those of Hayes et al. [5], and Neary and Sotiropoulos [6].

For the case of shear-thinning fluids (i.e., n<1), no recirculation zone is seen to occur in the side branch till Re = 13, 11 and 8 for the case of n=0.6, 0.4, 0.2 respectively. Therefore, the flow separation gets delayed with the decreasing shear-thinning tendency (or on increasing the power-law index). Similar to the case with Newtonian fluids the recirculation regions begin to occur beyond a critical limit. Figures 11 - 13 show that the size of recirculation region also increases on decreasing the power-law index (n) from 0.6 to 0.2. Overall, from Figs. 10-13, it is observed that for same Reynolds number the recirculation zones penetrate far much deeper in the side branch on decreasing the power-law index. This is in well agreement with the flow patterns for Newtonian/non-Newtonian fluids as presented by Matos and Oliveira [23].

A secondary recirculation zone is also observed near the junction in the main branch as the fluid gets diverted into side branch (Figs. 10-13) for Re= 30, 50, 100, 150 and 200.

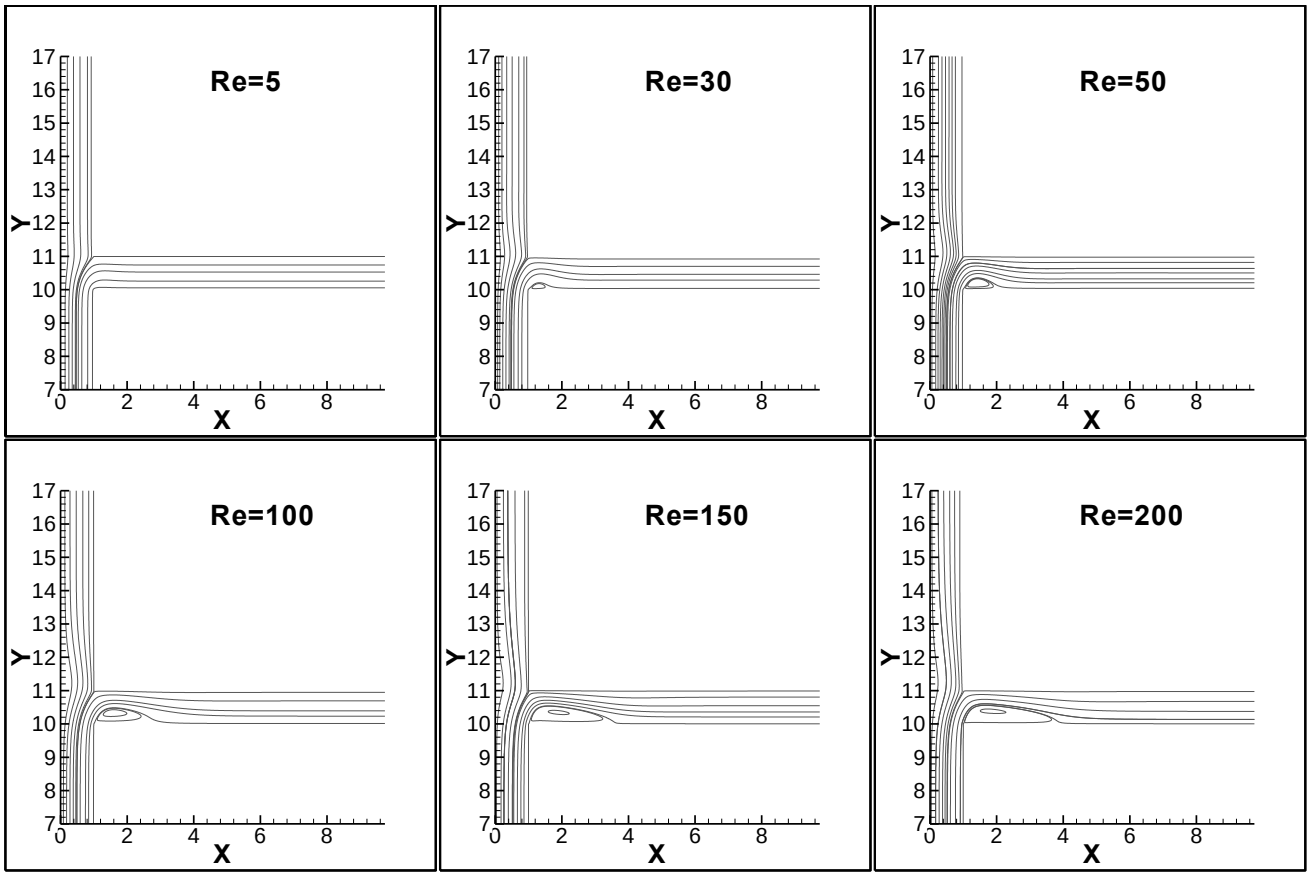

Figure 10: Stream function contours for fluid flow in a T-channel at different values of Reynolds number (Re) and power-law index, n = 1

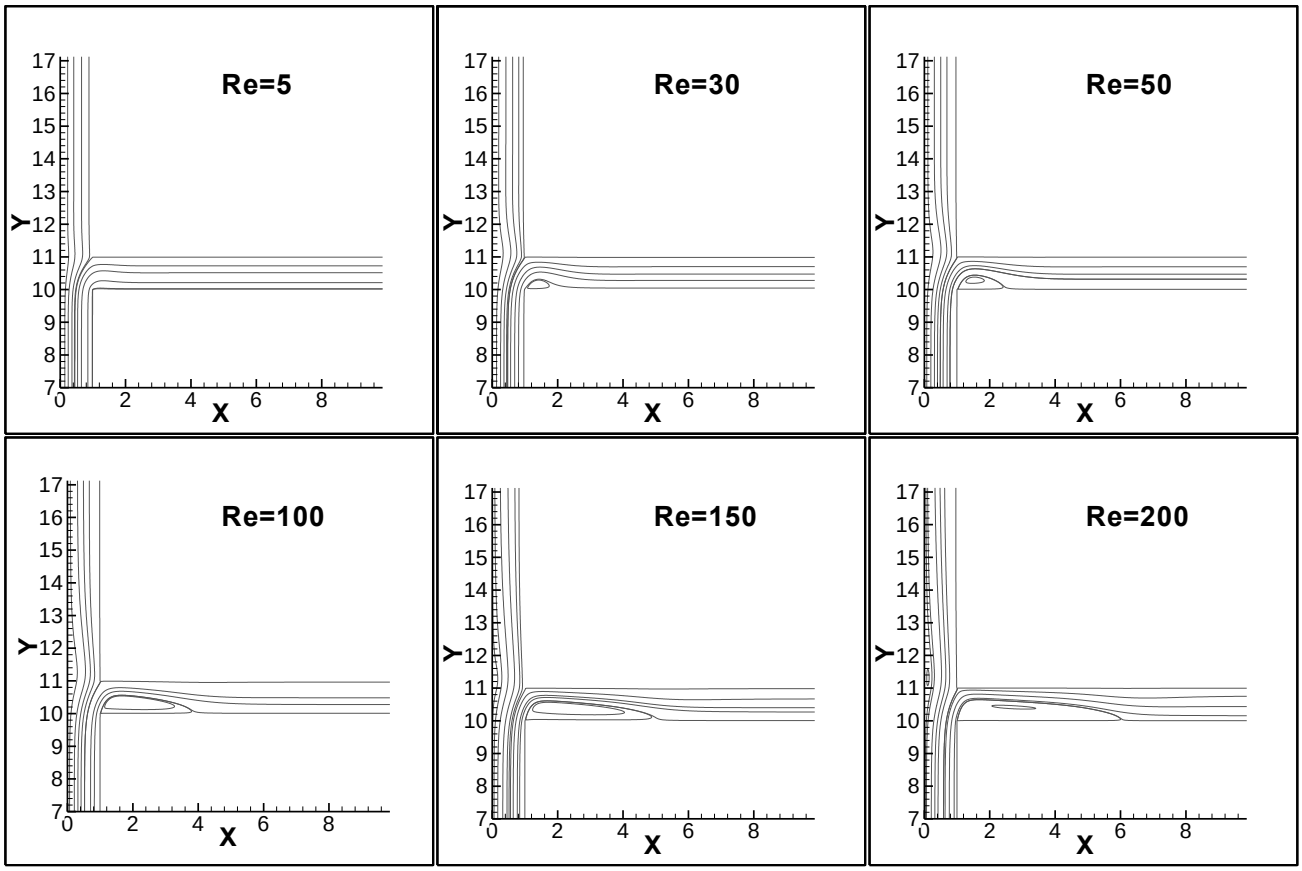

Figure 11: Stream function contours for fluid flow in a T-channel at different values of Reynolds number (Re) and power-law index, n = 0.6

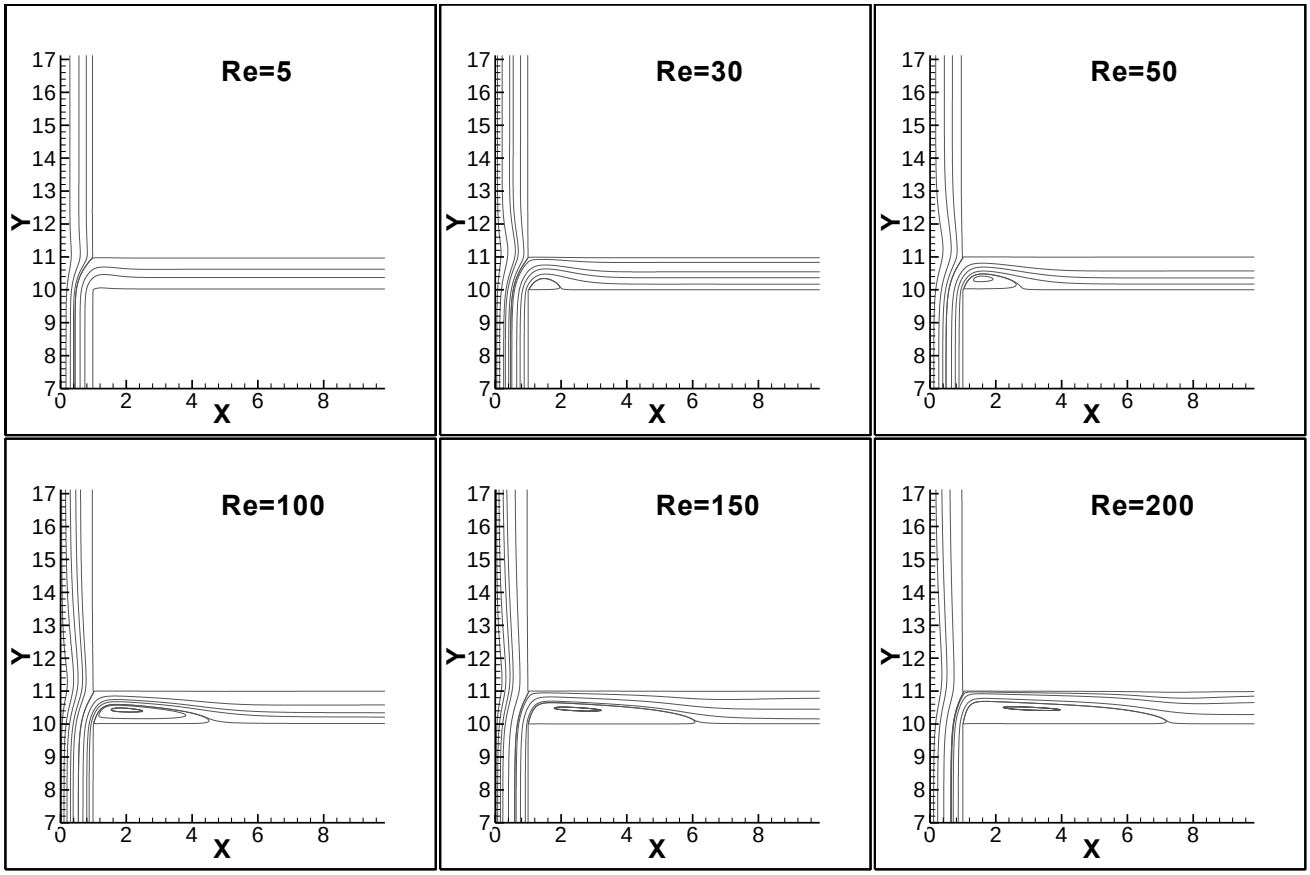

Figure 12: Stream function contours for fluid flow in a T-channel at different values of Reynolds number (Re) and power-law index, n = 0.4

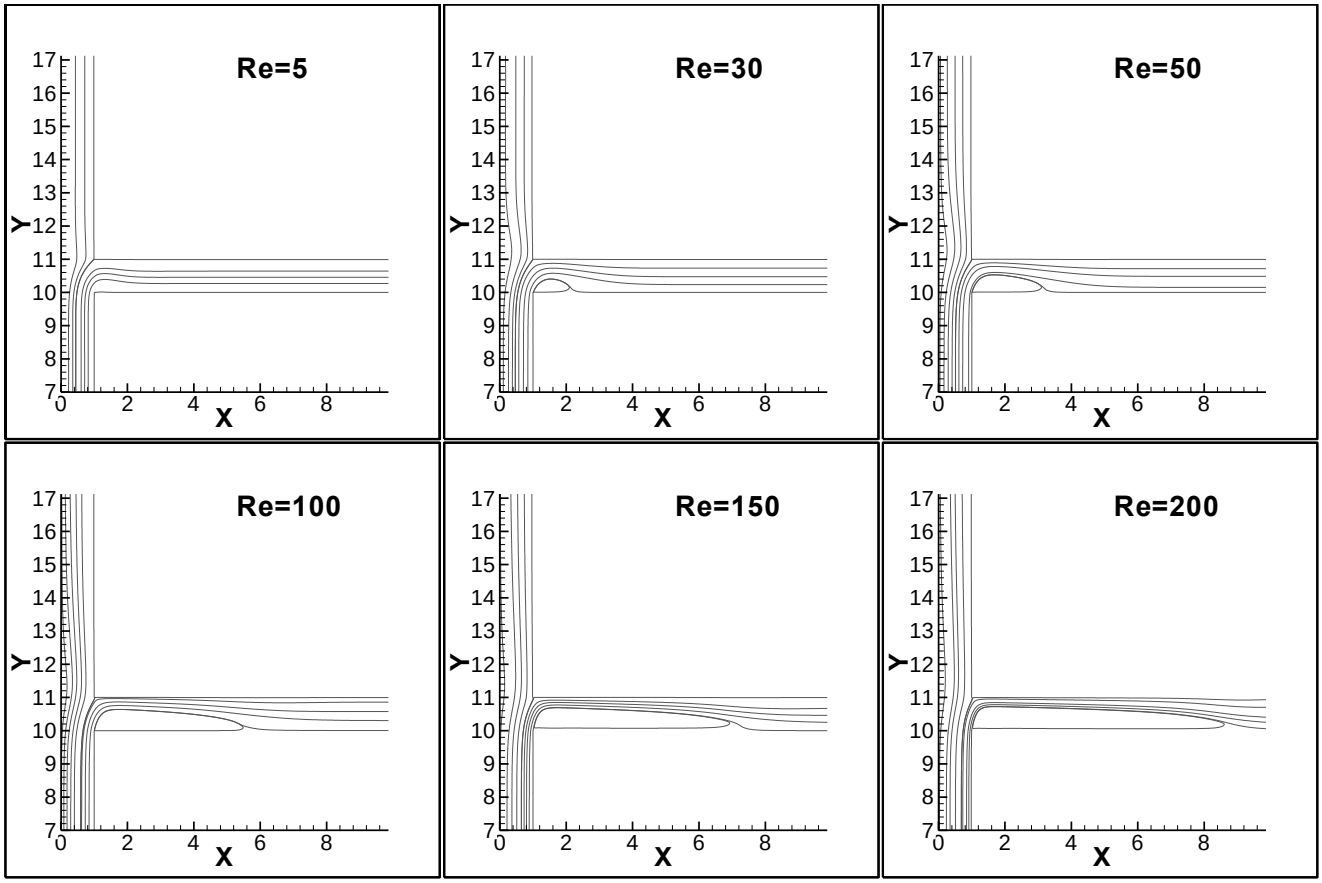

Figure 13: Stream function contours for fluid flow in a T-channel at different values of Reynolds number (Re) and power-law index, n = 0.2

4.3. Recirculation length

Recirculation length can be defined as the distance from the junction of the T-channel to the point of attachment of the fluid with the bottom wall of the side branch. The fluid when reaches junction experiences a change in direction of flow and loses its contact with the side walls of the channel. Thus a cavity is formed for a short distance when fluid enters the side branch. In this zone there is negligible fluid with a recirculating tendency, forming eddies. The velocity of fluid in this region is very small, so if the fluid contains suspended particles then this zone is very much susceptible to sedimentation. Prolonged sedimentation for a considerable period of time will reduce the channel conveyance width and ultimately block the flow in the side branch.

The variation of the non-dimensional recirculation length (L_r/D) in the side branch with Reynolds number and power-law index is shown in Fig. 14. The length of the recirculation region is observed to increase in a non-linear fashion on increasing Reynolds number for a particular power-law index. The recirculation length is also seen to increase with the decreasing power-law index for a fixed Reynolds number. Thus, the dimensionless considerations suggest the recirculation length to be a function of Reynolds number and power-law index.

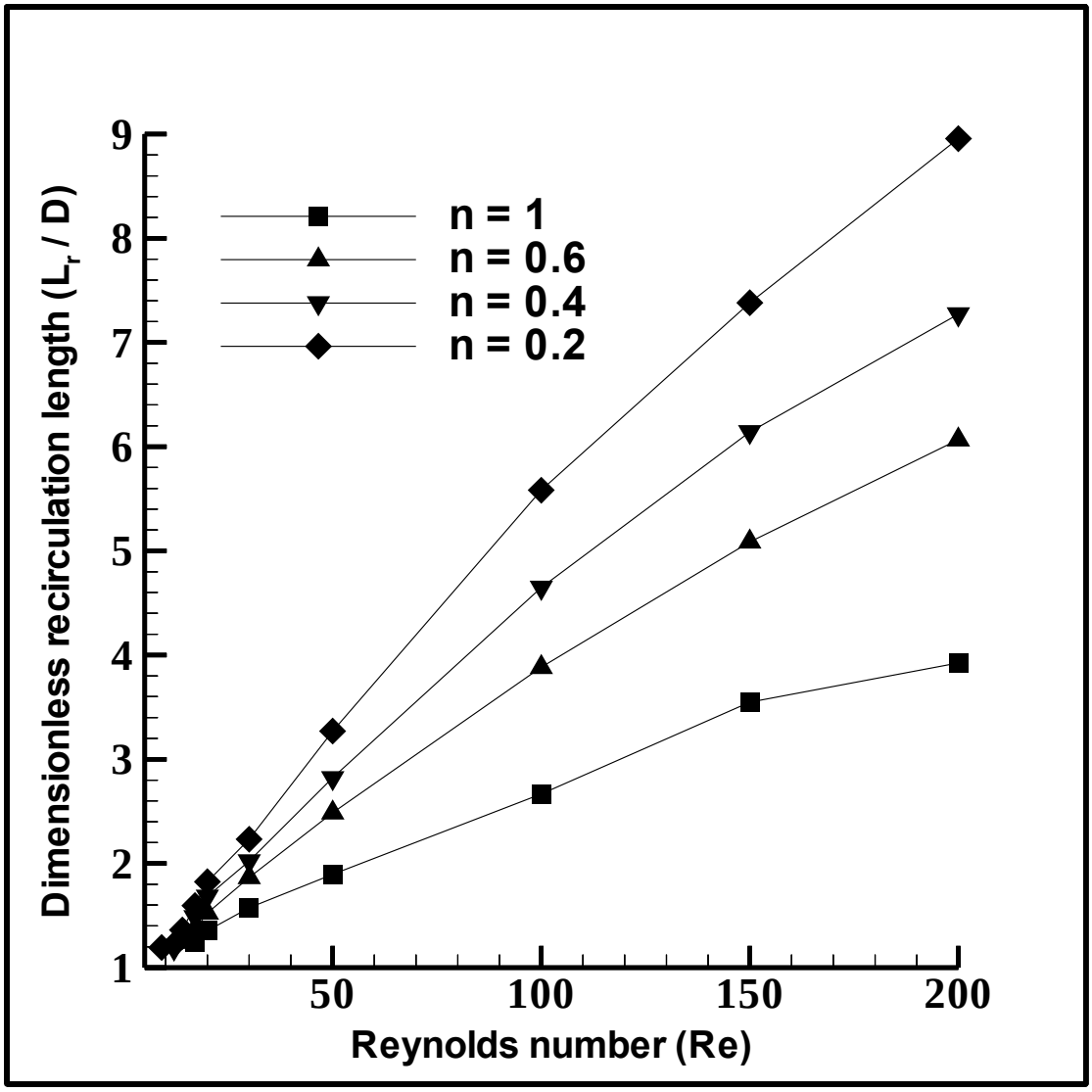

Figure 14: Variation of dimensionless recirculation length (L_r/D) with Reynolds number at different values of power-law index

To correlate dimensionless recirculation length with Re and *n*, an exponential form of equation is used to model the data obtained as:

$L_r/D = aRe^b + c$

where a, b and c are fitting coefficients and are given in Table 5. The maximum percentage deviation in the value of wake length from the above equation with the present computed results is also indicated in Table 5.

Table 5: Coefficients of exponential fit for the variation of dimensionless recirculation length with Reynolds number and power-law index

n	a	b	c	Max. error (%)
1	0.09495	0.6744	0.612	4.20
0.6	0.1374	0.7041	0.3623	1.89
0.4	0.183	0.6926	0.1612	3.85
0.2	0.2044	0.7142	0.01485	4.0

4.4. Onset of flow separation in side branch

The critical Reynolds number is the point beyond which the onset of recirculation region starts to develop in the side branch of the T-channel. This critical value of Reynolds number is determined for a range of values of power-law index studied here.

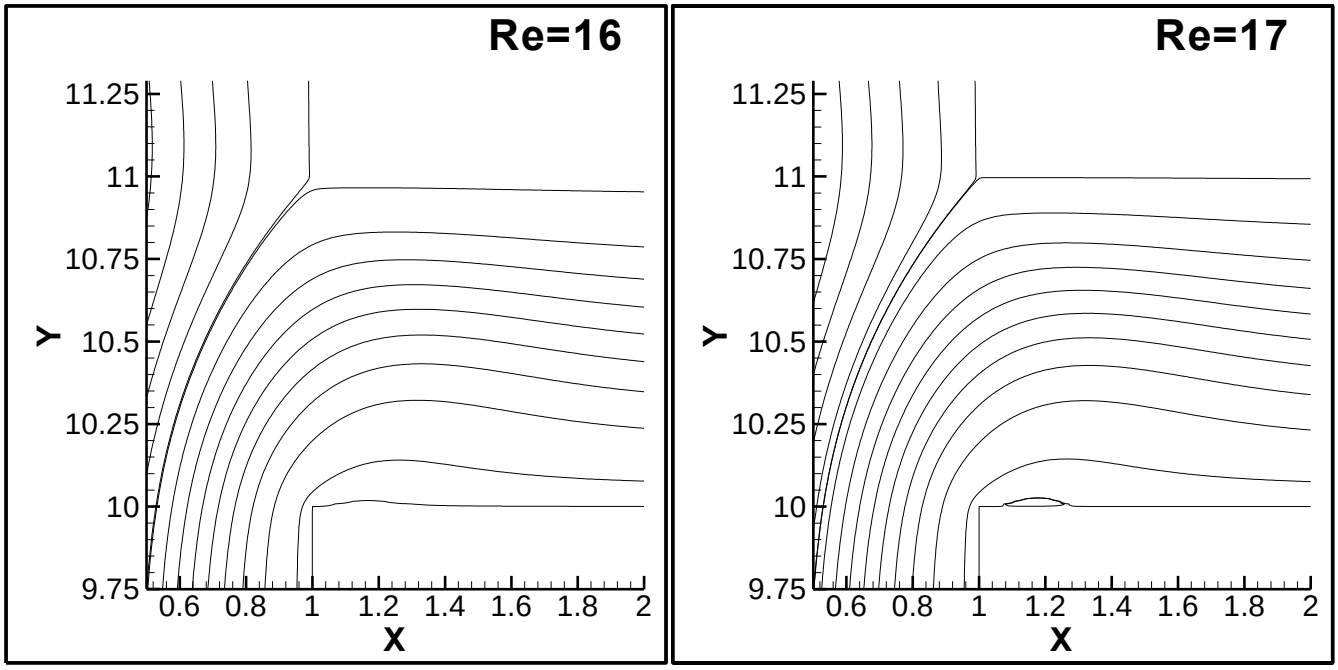

Figure 15: Flow patterns for critical Reynolds number at which onset of flow separation takes place for the case of *n*=1

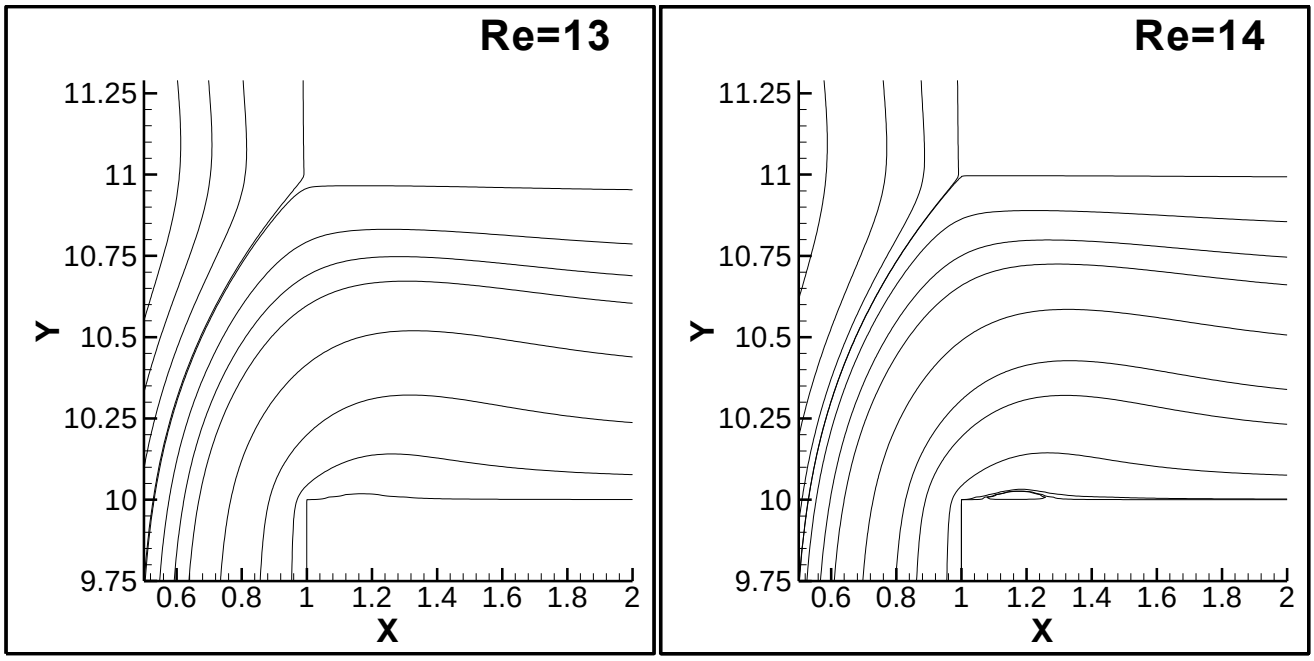

Figure 16: Flow patterns for critical Reynolds number at which onset of flow separation takes place for the case of *n*=0.6

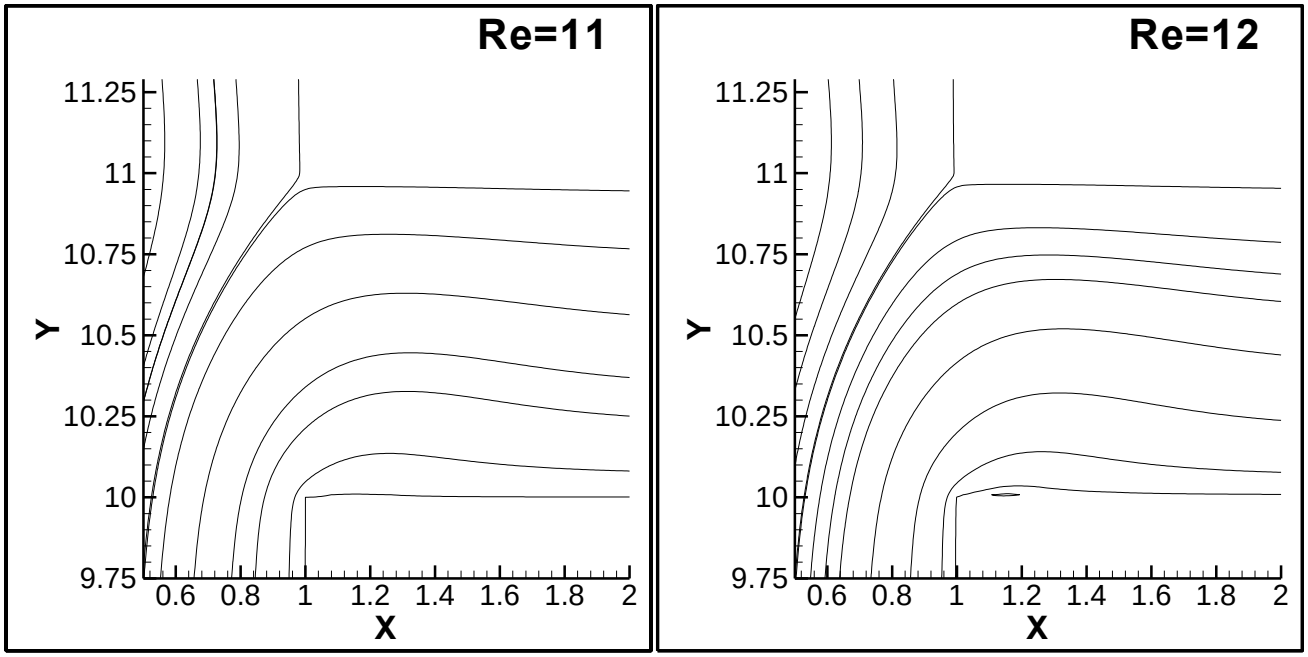

Figure 17: Flow patterns for critical Reynolds number at which onset of flow separation takes place for the case of *n*=0.4

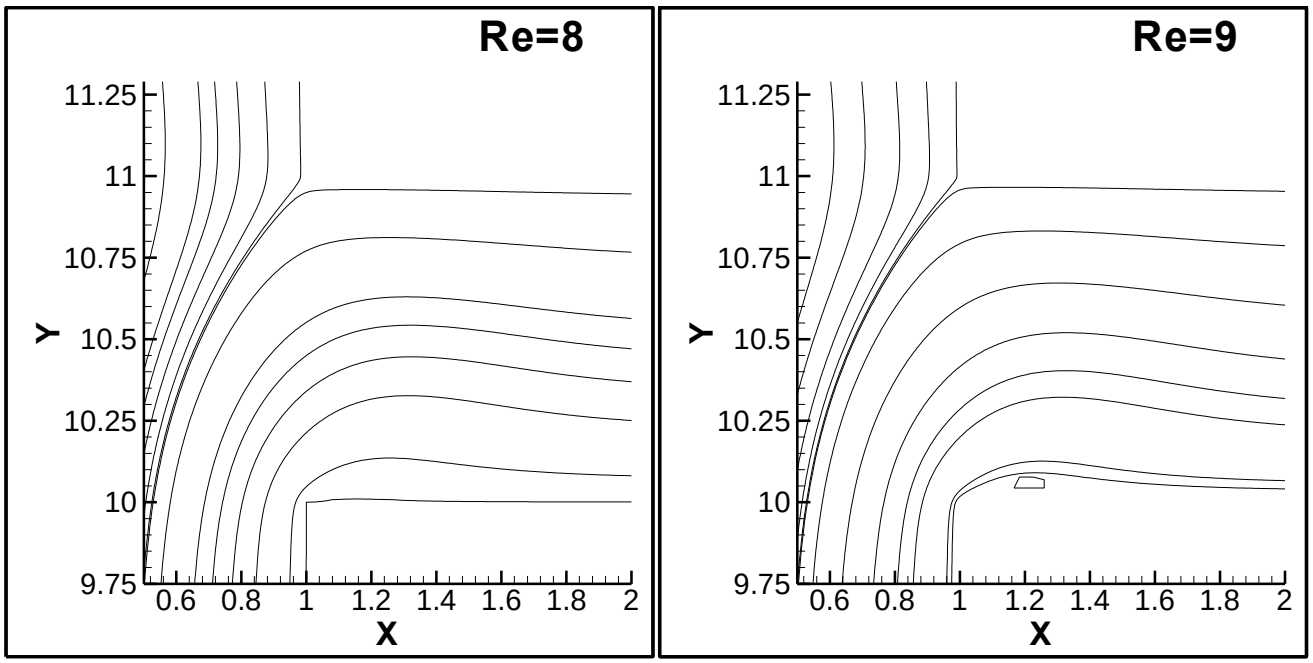

Figure 18: Flow patterns for critical Reynolds number at which onset of flow separation takes place for the case of *n*=0.2

Figure 15-18 depicts the flow patterns in a T-channel for critical Reynolds number at which onset of boundary layer separation occurs for the case of n = 1, 0.6, 0.4 and 0.2 respectively. For the case of Newtonian fluid (n=1) no recirculation region appear in the side wall up to Re=16 but as the Reynolds number is further increased to Re=17, wakes begin to appear in the side branch. This indicates the critical value of Reynolds number for the case of Newtonian fluid to be Re=17.

The critical Reynolds number for the case of Newtonian fluids is found to be in good agreement with the experimental results presented by Karino et al. [29, 30]. Similar computation was performed on shear-thinning fluids (n<1) for examining the onset of flow separation at different values of n. For n=0.6, the fluid maintain its contact with the lower wall of side branch and no wakes are observed till Re=13, but as we further carried our computation on Re=14 recirculation region begin to appear in side branch. Similarly, for n=0.4 and 0.2, no recirculation regions exist till Re=11 and Re=8 but begin to appear at Re=12 and Re=9 respectively.

Figure 19 shows the variation of critical Reynolds number with power-law index. The Reynolds number at which the onset of flow separation takes place in side branch decreases on decreasing the power-law index implying early recirculation zones with greater shear-thinning behaviour.

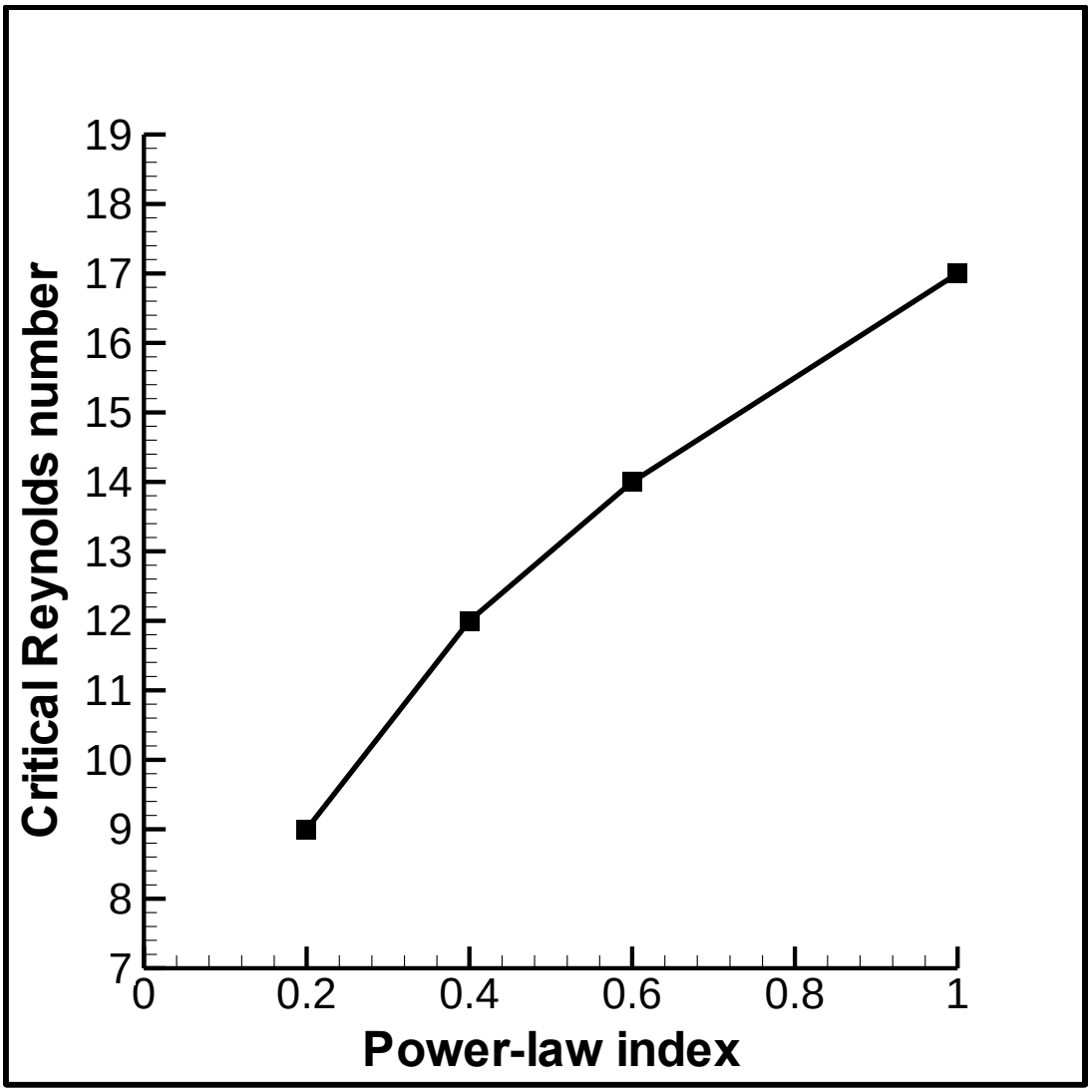

Figure 19: Critical Reynolds number for the onset of flow separation at different values of power-law index

4.5. Variation of viscosity along the side branch

The variation of viscosity along the bottom wall of a side branch of T-junction for Re= 5, 30, 50, 100, 150 and 200 for three different values of *n* (0.2, 0.4 and 0.6) is shown in Fig. 20-22.

For the case of Re = 5, no recirculation exists in flow pattern for any value of power-law index as seen from Figs 10-13. However, a peak in the power-law viscosity near the entrance of the side branch for Re = 5 is seen in Fig. 20 which is due to the small centrifugal force experienced by the fluid in this region. For the cases of Re = 30, 50, 100, 150 and 200, recirculation regions exist in the flow patterns of the side branch as seen in Figs. 10-13. A maximum is observed in the values of power-law viscosity in the bottom wall of side branch which then decreases to a constant value in the downstream of the side branch. The high values of viscosity for Re = 30, 50, 100, 150 and 200 at the bottom wall of the side branch are because of the recirculation of the fluid in that region. For the case of Newtonian fluids (n=1), the viscosity of the fluid remains constant throughout its span in the T-junction.

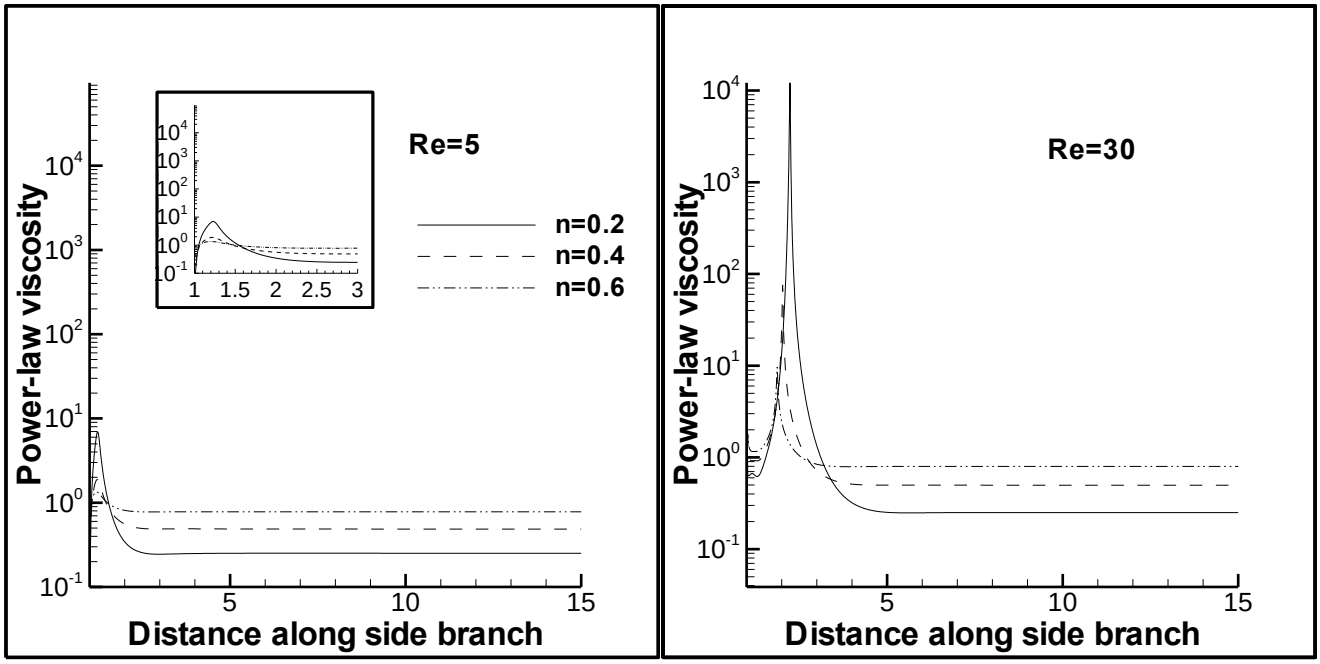

Figure 20: Variation of power-law viscosity along the lower wall of side branch for Re = 5 and 30 at different values of n

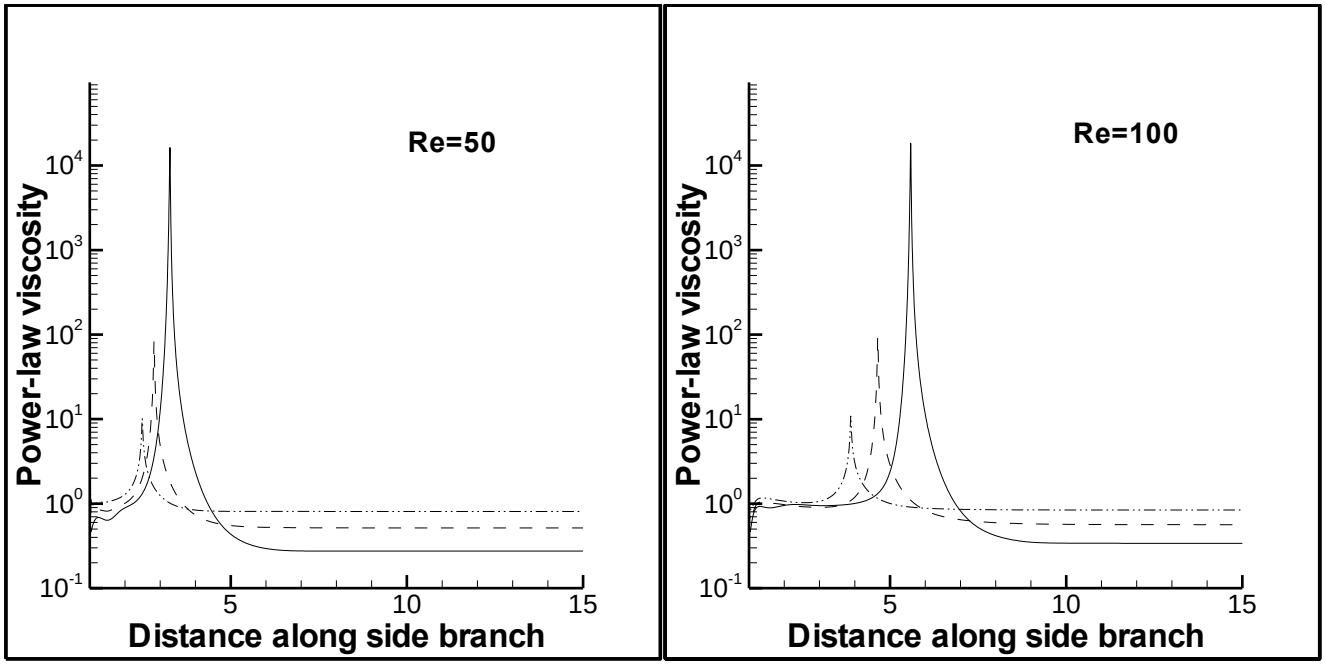

Figure 21: Variation of power-law viscosity along the lower wall of side branch for Re = 50 and 100 at different values of n

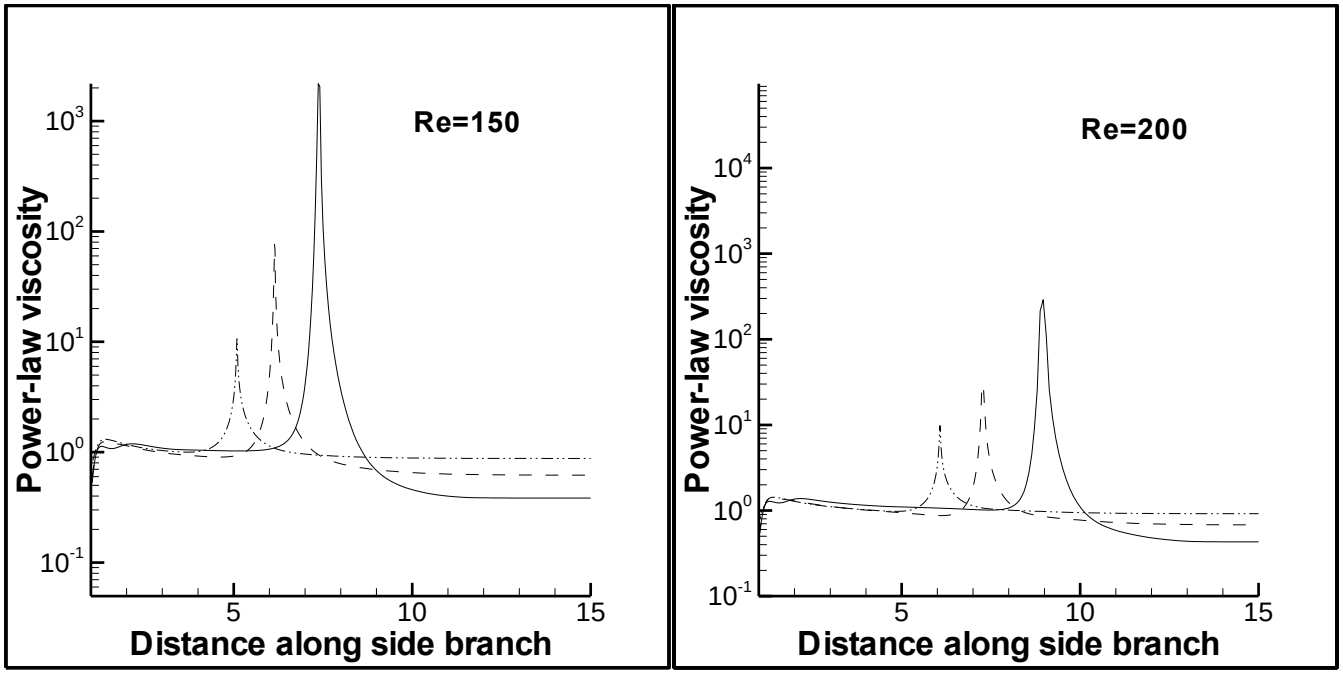

Figure 22: Variation of power-law viscosity along the lower wall of side branch for Re = 150 and 200 at different values of n

Chapter 5. Conclusions and Future Work

In the present work, the effects of Reynolds number (Re=5-200) and power-law index (n=0.2-1) on the flow of power-law fluids through a T-channel have been studied. The flow is observed to be steady for the range of settings investigated here. The numerical scheme has been extensively validated against the previous numerical and experimental studies, and the grid and computational domain were chosen after extensive testing for domain and grid independence. Detailed observations of flow pattern, recirculation length, critical Reynolds number for the onset of boundary layer separation and viscosity variation along the bottom wall of the side branch have been presented. The results showed that the length of recirculation zone increases on increasing Reynolds number for a particular power-law index. It also increases on decreasing the power-law index for a fixed Reynolds number. The critical Reynolds number at which the onset of flow separation takes place in the side branch decreases on decreasing the power-law index (or with increasing shear-thinning tendency).

Although, the current work numerically investigates into the problem of 2-D laminar flow of non-Newtonian shear-thinning fluids in a T-channel, further experimentation of the problem under consideration is necessary. The fluid flow characteristics may be visualized via some commercially available fluid flow measurement techniques viz. Particle Image Velocimetry (PIV), Laser Doppler Velocimetry etc. Furthermore, the flow disturbances in shear-thinning fluids exist up to a larger distance in side branch than in Newtonian fluids. So, at low values of power-law index the 2D simulation may fail to resemble actual 3D behaviour of flow at high Reynolds number. Thus, it is advisable to perform 3D simulations for capturing the exact flow characteristics of flow in a T-channel for shear-thinning fluids at Reynolds number higher than that used in this study.

References

[1] Ramamurthy, A.S., Qu Junying and Vo Diep, "Numerical and experimental study of dividing open channel flows." J. Hydraul. Res. 133, (2007), 1135-1144.

[2] Neary, V.S., Sotiropoulos, F., and Odgaard, A.J., "Three-dimensional numerical model of lateral-intake inflows." J. Hydraul. Eng., 125, (1999), 126–140.

[3] Grace, J.L. and Priest, M.S., "Division of flow in open channel junctions." Bulletin No. 31, Engineering Experimental Station, Alabama, Polytechnic Institute, Auburn, Ala, (1958).

[4] Law S.W., and Reynolds A. J., "Dividing flow in an open channel." J. Hydr. Div. 92, (1966), 4730–4736.

[5] Hayes, R.E., Nandakumar, K. and Nasr-El-Din, H., "Steady laminar flow in a 90 degree planar branch." Comput. Fluids 17, (1989), 537-553.

[6] Neary, V.S. and Sotiropoulos, F., "Numerical investigation of laminar flows through 90-degree diversions of rectangular cross-section. "Iowa Institute of Hydraulic Research, The University of Iowa, Iowa City, IA 52242, U.S.A (1995).

[7] Weber, L.J., Schumate, E.D. and Mawer, N., "Experiments on flow at a 90° open-channel junction." J. Hydraul. Eng. 127, (2001), 340-350.

[8] Huang, J., Weber, L.J., and Lai, Y.G., "Three-dimensional numerical study of flows in open-channel junctions." J. Hydraul. Eng. 128, (2002), 268–280.

[9] Shamloo, H. and Pirzadeh, B., "Investigation of characteristics of separation zones in T-Junctions." WSEAS Trans. Mathematics 7, (2008), 303-312.

[10] Shettar A.S. and Murthy K.K., "A Numerical study of division flow in open channels." J. Hydraul. Res. 34, (1996), 651-675.

[11] Kasthuri B. and Pundarikhanthan N.V, "Discussion on separation zone at open channel

junction". J. Hydraul. Eng. 113, (1987), 543-548.

[12] Mathioulakis D.S., Pappou Th. and Tsangaris S., "An experimental and numerical study of a 90° bifurcation." Fluid Dyn. Res. 19, (1997), 1-26.

[13] Yanase, S., Kaga, Y. and Daikai, R., "Laminar flows through a curved rectangular duct over a wide range of the aspect ratio." Fluid Dyn. Res. 31 (2002), 151-183.

[14] Liepsch, D., Moravec, S., Rastogi, A.K. and Vlachos, N.S., "Measurements and calculation of laminar flow in a ninety degree bifurcation." J. Biomech. 15, (1982), 473-485.

[15] Bramley, J.S. and Dennis, S.C.R., "The numerical solution of two-dimensional flow in a branching channel." Comput. Fluids 12, (1984), 339-355.

[16] Ehrlich L.W. and Friedman M.H., "Computational aspects of aortic bifurcation flows." Comput. Fluids 13, (1985), 177-183.

[17] Miranda, A.I.P., Oliveira, P.J. and Pinho, F.T., "Steady and unsteady laminar flows of Newtonian and generalized Newtonian fluids in a planar T-junction." Int. J. Numerical Methods Fluids 57, (2008), 295–328.

[18] Khodadadi, J.M., Vlachos, N.S., Liepsch, D. and Moravec, S., "LDA measurements and numerical prediction of pulsatile laminar flow in a plane 90-degree bifurcation." J. Biomechanical Engineering 110, (1988), 129–136.

[19] Khodadadi, J.M., Nguyen, T.M. and Vlachos, N.S., "Laminar forced convective heat transfer in a two-dimensional 90^{o} bifurcation." Numer. Heat Transfer 9, (1986), 677-695.

[20] Khodadadi, J.M., "Wall pressure and shear stress variations in a 90-deg bifurcation during pulsatile laminar flow." J. Fluids Engineering 113, (1991), 111–115.

[21] Benes L., Louda Petr., Kozel K., Keslerova R. and Stigler J., "Numerical simulations of flow through channels with T-junction." Appl. Math. Comput. 219, (2011), 7225–7235.

[22] Moshkin, N. and Yambangwi, D., "Steady viscous incompressible flow driven by a pressure difference in a planar T-junction channel." Int. J. Comput. Fluid Dyn. 23,

(2009), 259–270.

[23] Matos, H.M. and Oliveira, P.J., "Steady and unsteady non-Newtonian inelastic flows in a planar T-junction." Int. J. Heat Fluid Flow 39, (2013), 102-126.

[24] Bird, R.B., Stewartm W.E. and Lightfoot, E.N., "Transport Phenomena", 2nd Edition, John Wiley & Sons, Inc., New York (2002).

[25] Chhabra, R.P. and Richardson, J.F., "Non-Newtonian Flow and Applied Rheology", 2nd Edition, Butterworth-Heinemann, Oxford, U.K. (2008).

[26] Bharti, R.P. and Chhabra, R. P., "Two-Dimensional steady Poiseuille flow of power-law fluids across a circular cylinder in a plane confined channel: wall effects and drag coefficients." Ind. Eng. Chem. Res. 46, (2007), 3820-3840.

[27] Reid, W.H., "On the stability of viscous flow in a curved channel". Proc. R. Soc. Lond. A244, (1958), 186-198.

[28] Roache, P.J., "Verification and Validation in Computational Science and Engineering", Hermosa Publishers, Albuquerque, New Mexico (1998).

[29] Karino, T., Kwong, H.H.M. and Goldsmith, H.L., "Particle flow in models of branching vessels: I. Vortices in 90^{o} T-junctions." Biorheology 16, (1979), 231-248.

[30] Karino, T. and Goldsmith, H.L., "Particle flow in models of branching vessels: II. Effects of branching angle and diameter ratio on flow patterns." Biorheology 22, (1985), 87-104.

[31] FLUENT user's guide manual-version 6.1., Fluent Incorporated, N.H., (2003).

[32] Kumar, A. and Dhiman, A.K., "Effect of a circular cylinder on searated forced convection ata backward-facing step." Int. J. Thermal Sciences 52, (2012), 176-185.